Acta Geologica Sinica (English Edition), 2021, 95(2): 500–516

U-Pb Zircon and Re-Os Molybdenite Geochronology of the W-Mo Mineralized Region of South Qinling, China, and their Tectonic Implications

HAN Ke[1], YANG Xingke[1, 2, *], CHAO Huixia[1, 2], HE Hujun[1, 2], RUAN Shiqi[1], GAO Yunfeng[1], ZHANG Weisheng[1], ZHU Wei[3] and JIN Gang[1]

[1] *School of Earth Science and Resources, Chang'an University, Xi'an 710054, China*
[2] *Key Laboratory of West Mineral Resources and Geology Engineering Ministry of Education, Chang'an University, Xi'an 710054, China*
[3] *Shaanxi Mineral Resources and Geological Survey, Xi'an 710054, China*

Abstract: A W-Mo mineralized region is located along the northern margin of the South Qinling tectonic belt of China. W-Mo mineralization occurs mainly in Cambrian–Ordovician clastic and carbonate rocks, and the ore bodies are structurally controlled by NW–SE- and NNE–SSW-striking faults. Evidence for magmatism in the area is widespread and is dominated by intermediate–felsic intrusives or apophyses, such as the Dongjiangkou, Yanzhiba, Lanbandeng, and Sihaiping granitic bodies. Quartz-vein-type mineralization and fault-controlled skarn-type mineralization dominate the ore systems, with additional enrichment in residual deposits. At present, there are few or insufficient studies on (1) the age of mineralization, (2) the relationship between intermediate–felsic granite and W-Mo mineralization, (3) the source of ore-forming materials, and (4) the metallogenic and tectonic setting of the mineralized area. In this paper, we present geochronology results for numerous intrusive granitic bodies in the South Qinling tectonic belt. U-Pb zircon geochronology of the Lanbandeng monzogranite and Wangjiaping biotite monzogranite yields ages of 222.7 ± 2.3 and 201.9 ± 1.8 Ma, respectively. In contrast to the Late Triassic age of the Lanbandeng monzogranite, the age of the newly discovered Wangjiaping biotite monzogranite places it at the Triassic–Jurassic boundary. Re-Os molybdenite geochronology on the Qipangou W-Mo deposit yielded a model age of 199.7 ± 3.9 Ma, indicating the deposit formed in the early Yanshanian period of the Early Jurassic. Granitoid intrusions in the mineralized area are characterized by composite granite bodies that crystallized at ca. 240–190 Ma. While there were multiple stages of intrusion, most occurred at 210–220 Ma, with waning magmatic activity at 200–190 Ma. The Re-Os age of molybdenite in the region is ca. 200–190 Ma, which may represent a newly discovered period of W-Mo metallogenesis that occurred during the final stages of magmatism. The heat associated with this magmatism drove ore formation and might have provided additional ore-forming components for metallogenesis (represented by the Wangjiaping biotite monzogranite). Ore materials in the mineralized area were derived from mixed crustal and mantle sources. Enrichment of the region occurred during intracontinental orogenesis in the late Indosinian–Yanshanian, subsequent to the main Indosinian collision. At this time, the tectonic environment was dominated by extension and strike-slip motion.

Key words: U-Pb zircon geochronology, Re-Os molybdenite geochronology, tungsten-molybdenum mineralized area, intracontinental orogeny, South Qinling

Citation: Han et al., 2021. U-Pb Zircon and Re-Os Molybdenite Geochronology of the W-Mo Mineralized Region of South Qinling, China, and their Tectonic Implications. Acta Geologica Sinica (English Edition), 95(2): 500–516. DOI: 10.1111/1755-6724.14653

1 Introduction

China has one of the world's largest W reserves. According to USGS (2012), China's W output accounted for 83.3% of global production, and its reserves account for 61.3% of the global total. Globally, W is predominantly hosted in wolframite (30%) and scheelite (70%), with the latter contained within both skarn- and porphyry-type deposits. Since the onset of the 21st century, China has discovered numerous additional W deposits in the metallogenic belts of the Liaoji, Fujian–Zhejiang, Nanling, Jiuling terranes, East Qinling, East Kunlun, Beishan, and North Qilian. While the majority of these recently discovered W deposits are hosted in scheelite, the Nanling and Jiuling regions contain wolframite-hosted W (Huang, 2009). Of the 29 large to superlarge W deposits presently documented in China, 20 are classified as scheelite deposits (Li, 2009). However, given limitations associated with mineral processing capabilities and the structure of these deposits, >90% of Chinese W output has been derived from the less abundant wolframite deposits. As a consequence, the wolframite-hosted W reserves in China are highly depleted.

Therefore, to maximize future W output, research into the under-utilized scheelite deposits that are particularly

* Corresponding author. E-mail: xky61@163.com

prevalent in northwestern China is required (Mao et al., 2000; Nie et al., 2004; Zhang et al., 2010). Theoretical and prospecting progress has most notably been made in the Nanling W-Sn-Mo ore regions in Jiangxi Province. Until 2016, Jiangxi Province has 158 proven W deposits including 15 large and 24 medium deposits, with a total wolframite quantity of 5.2548 million tons. This accounts for 43% of the total known W in China. The main mineralization types include quartz vein-, skarn-, greisen-, altered granite-, and porphyry-type, with some additional mineralization in cryptoexplosive breccia. These mineralization varieties have led to the development of a "five-floor and basement" prospecting model (Xu et al., 2008). In Nanling and adjacent regions, peak W-Sn metallogenesis occurred at 160–150 Ma during the second period of large-scale Mesozoic mineralization in South China. This mineralization formed in a back-arc extensional environment associated with continuous low-angle subduction of the Paleo-Pacific Plate (Mao et al., 2007, 2009a, 2011a). Feng et al. (2007a, 2007b, 2010) further showed that these large-scale W-Sn deposits formed in an extensional intraplate setting in the Middle–Late Jurassic by determining high-precision metallogenic ages of several W deposits in southern Jiangxi Province.

The Qinling orogenic belt divides the South China and North China blocks. As a consequence of protracted subduction, collision, and magmatism over three billion years, the structure of the region is complex (Fig. 1). Granites with a wide range of genetic origins are extensive, and the region has experienced multiphase tectonism that resulted in a range of crustal structures and compositions. The Qinling orogenic belt comprises the Shangdan suture belt, Mianlue suture belt, southernmost margin of the North China Block, Qinling microblock, and northernmost margin of the Yangtze Block (Zhang et al., 1995, 2001). The South Qinling belt is located between the Mianlue and Shangdan suture belts, and was accreted during the Late Triassic (220–210 Ma) during a period of structural adjustment after continental collision. At this time, extensional tectonics dominated over collisional tectonics. Crustal-scale decompression partial melting in South Qinling resulted in both the intrusion of voluminous

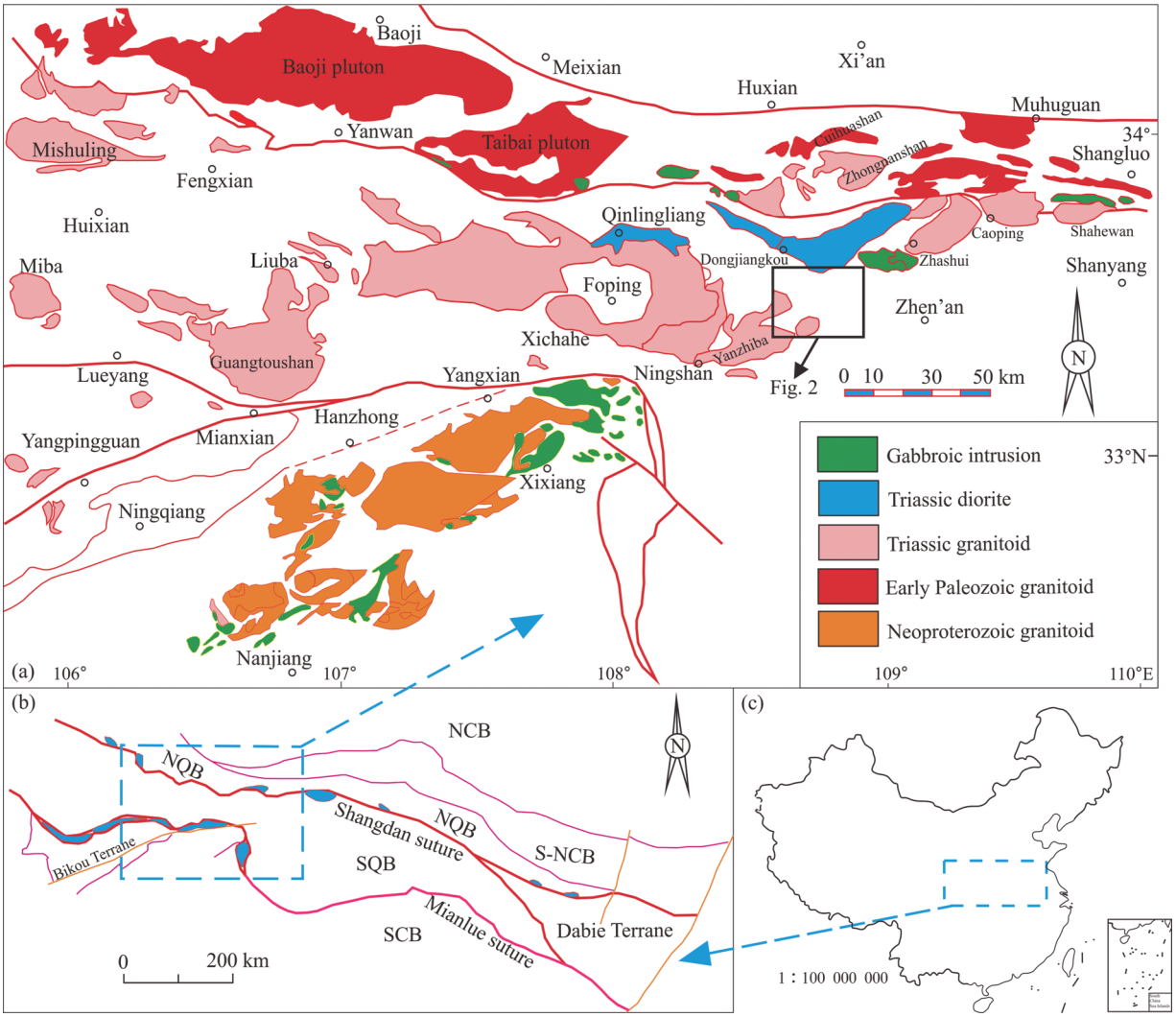

Fig. 1. Simplified maps of (a) granitoid distribution in the South Qinling belt; (b) tectonic divisions of the Qinling orogenic belt; (c) location of the Qinling orogenic belt within China (modified after Dong et al., 2012).

China basemap after China National Bureau of Surveying and Mapping Geographical Information. NCB, North China Block; S-NCB, Southern margin of the North China Block; NQB, North Qinling belt; SQB, South Qinling belt; SCB, South China Block.

granites and Au, W, Mo, Pb, and Zn mineralization. During crustal thinning in the Mesozoic, the development of crustal-scale faults and associated magmatism facilitated exchange of material between the crust and mantle. As a consequence, this enabled the migration and enrichment of ore-forming elements in a range of rock series at different levels (Wang and Chen, 1997; Wang et al., 2002; Yao et al., 2002; Du et al., 2003; Mao et al., 2005; Zhu et al., 2009; Yan et al., 2014).

The W-Mo enriched region is located in the South Qinling tectonic belt, Shaanxi Province, China. It covers an area of ca. 2120 km^2 and is 69 km long and 47 km wide. Au, Mo, Pb, Zn, Ag, Cu, and W anomalies have been identified both in the granitoid intrusions of Dongjiangkou, Sihaiping, Lanbandeng, and Caoping, and in country rocks of Lower Cambrian–Middle Ordovician and Middle–Upper Devonian. Given the high abundance of ore minerals and the large scale over which metallogenesis has occurred in the W-Mo mineralized area, numerous potential ore prospecting areas have been described. The region is closely related to the structure and setting of Indosinian felsic igneous rocks, and contains numerous quartz vein-, skarn-, and porphyry skarn-type W -Mo deposits (e.g., the Xinpu, Yueheping, Daxigou, Shentangou, Yangsi, Liyuantang, Jinpen, Dongyang, Qipangou, Yanggou, and Guilingou deposits). The ore bodies are controlled by (N)NE–(S)SW- and near E–W-striking faults, and are largely contained within granite, monzogranite, and granodioritic porphyry which have a Late Triassic–Early Jurassic mineralization age (Li S Q et al., 2010; Dai et al., 2015; Zhang et al., 2015; Dai et al., 2018).

While our understanding of the mineralized area is improving, there are few studies on (1) the age of mineralization, (2) the relationship between intermediate–felsic granites and W-Mo mineralization, (3) the source of ore-forming materials, and (4) the tectonic setting of metallogenesis. By utilizing previous research, this contribution presents U-Pb zircon geochronology of both the Lanbandeng monzogranite and the newly discovered Wangjiaping biotite monzogranite. We also present results of Re-Os geochronology conducted on molybdenite from the Qipangou W-Mo deposit. These approaches permit us to determine the age of mineralization, and to shed light on the source of ore-forming materials. Based on the above research and combined with the formation and evolution of the South Qinling orogenic belt, we have analyzed the spatial-temporal coupling among tectonism, magmatism, and mineralization in the intracontinental orogenic stage during the late Indosinian.

2 Regional Geology

The ore-bearing region is located along the northern margin of the South Qinling tectonic belt, south of the Shangdan mélange belt. Sediments comprise mainly Upper Paleozoic and Devonian shallow shelf facies (predominantly fine clastic carbonates), local Sinian system sediments, and Cambrian–Ordovician clastics and carbonates. Faults strike WNW–ESE (e.g., the Shanyang–Fengzhen, Yungaisi, and Zhen'an–Banyanzhen faults) and NNE–SSW (e.g., the Xunyangba, Shentangou, Huangjinmei, Yanggou, and Yangmugou faults). The WNW–ESE-striking faults exhibit ductile structures and form thrust nappes, and the NNE–SSW-striking faults are sinistral and linked to numerous secondary transtensional faults. The two discrete fault network orientations form an orthogonal fracture pattern that most likely controlled mineralization (Fig. 2). Intermediate–felsic intrusions (e.g., the Jinning, Caledonian, Indosinian, and Yanshanian bodies) were emplaced in stages, and there are numerous minor intrusions and apophyses (e.g., the Dongjiangkou, Yanzhiba, Lanbandeng, and Sihaiping bodies) (Fig. 2).

The Dongjiangkou composite granite body is situated between the Shangdan and Shanyang–Fengzhen faults. It is elongate with a NE–SW-strike, and obliquely intrudes into pre-Devonian strata. The granite contains mafic enclaves, and the inner zone is foliated parallel to the intrusion interface, which has a chilled margin. Wall rock xenoliths are present but rare, and the outer contact is associated with variably wide hornfelsic zones that formed by thermal metamorphism. The Dongjiangkou composite granite body can be subdivided into the Xiaochuanjie and Liulijie granitoid intrusions. The former is a medium–fine-grained quartz monzonite, and the latter is a medium–coarse-grained porphyritic biotite monzogranite.

The irregularly shaped Yanzhiba composite granite body is southwest of the main study area, strikes NE–SW, and was intruded into Paleozoic strata. Granite veins are common towards the edge of the body, and the intrusive relationship is preserved between the granite and wall rock. Hornfelsic zones at the margin are several to dozens of meters wide, and are exposed across an area of ca. 470 km^2. The Yanzhiba composite granite body can be divided into four granitoid intrusions, each of which comprises multiple intrusive bodies: (1) Jiujianwu (a medium–coarse -grained porphyritic biotite K-feldspar granite); (2) Yingzuishi (a medium–coarse-grained porphyritic biotite monzogranite); (3) Tianwan (a medium–fine-grained biotite monzogranite); and (4) Xiaoshuihe (a fine-grained biotite monzogranite). W-Mo mineralization accompanies the hornfels and skarns developed at the edge of the Yanzhiba composite granite body.

The Lanbandeng granitoid intrusion is exposed over ca. 10 km^2 near Dazengxigou–Yuanjiayuanzi, in the center of the study area. The intrusion is largely granitic, and wall rocks in the outer contact zone are hornfelsic. Thermal metamorphism in the Devonian also resulted in the development of marble, realgar, and Pb-Zn ore in distal regions.

The Sihaiping granitic intrusion is located in the Yangsimiao–Wenjiajie region, in the central–southern part of the study area. It strikes NE–SW with an elliptical shape that intrudes into Paleozoic strata, and is composed of gray–white, fine-grained, porphyritic, biotite K-feldspar granite and medium–coarse-grained porphyritic biotite monzogranite. Hornfels and skarns are developed at the edge of the Sihaiping instrusion, which is accompanied by W-Mo mineralization.

The Wangjiaping granitic intrusion is associated with the Lijiawan–Yaowan W-Mo deposit, and while it does not crop out at the surface, its structure has been

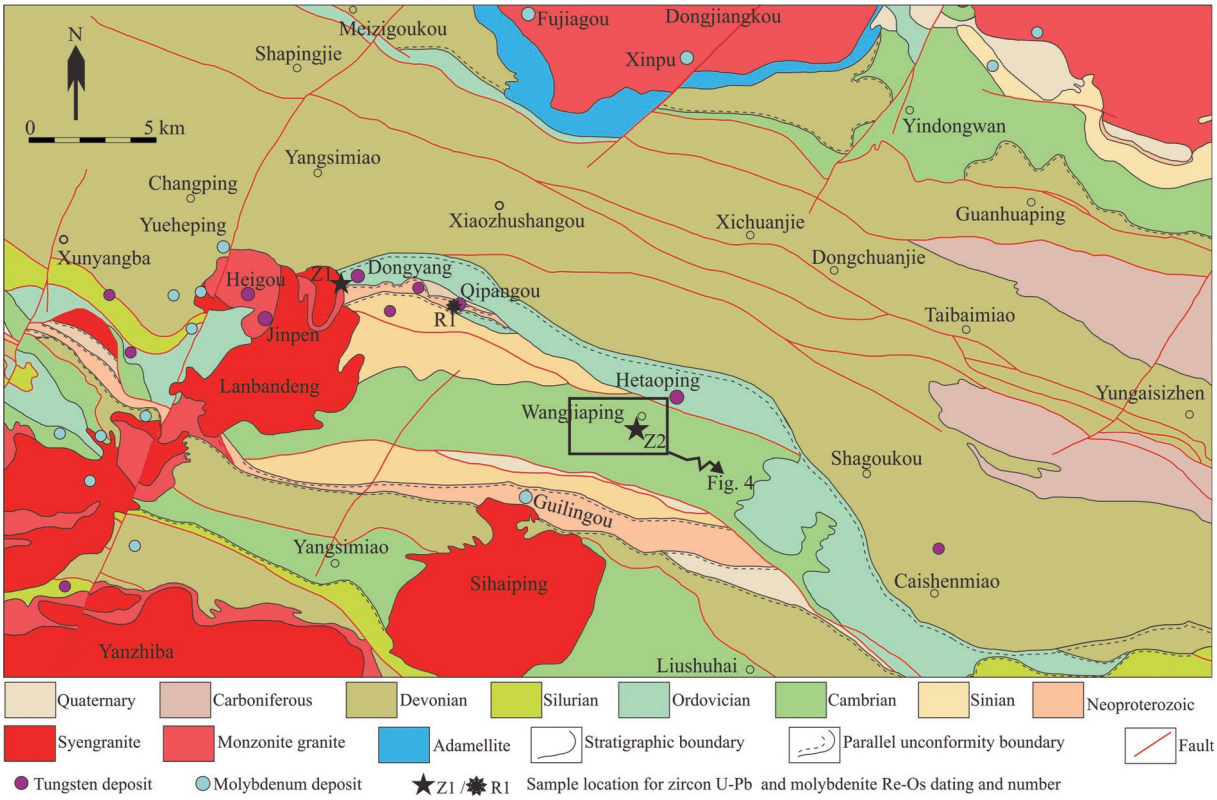

Fig. 2. Geological map of the W-Mo mineralized region of South Qinling, modified after unpublished data (Shaanxi Mineral Resources and Geological Survey, 2018).

tcharacterized by five cores drilled to a depth of 550–700 m. The intrusion is located to the south of the Yuehe Fault and southeast of the semi-circular ring, which comprises numerous granitoid intrusions (the Dongjiangkou, Lanbandeng, Yanzhiba, and Sihaiping intrusions in the north, west, southwest, and south, respectively). Its predominant lithology is a gray–white, medium–fine-grained biotite monzogranite.

3 Characteristics of Alteration and W-Mo Mineralization

Numerous W-Mo deposits (including the Yueheping, Jinpen, Dongyang, Qipangou, Hetaoping, and Guilingou deposits) have been identified surrounding the intermediate–felsic intrusions in the mineralized area (Fig. 2). They are predominantly located within Cambrian–Ordovician clastic and carbonate rocks, and the ore is mainly hosted in quartz veins and fault-controlled skarns, followed by residual deposit.

The Lanbandeng granitoid intrusion is irregularly shaped, intrudes Paleozoic strata, and shows intrusive contacts with the country rock (Fig. 3a) and a variety of contact relationships between the different phases of the intrusion. Biotite hornfels, skarn assemblages, and W-Mo mineralization are developed within a zone, commonly 0–200 m wide, but wider in places, at the margin of the intrusion (Fig. 3b–d, f). Early alteration formed tremolite, diopside, epidote and fluorite, and late alteration formed chlorite, carbonates, sericite, quartz veins, pyrite, limonite, and silicification (Fig. 3c, e). The scheelite mineralization is associated with the early alteration mineral assemblage (Wang et al., 2017). The Yueheping molybdenite ore body is located on the northern margin of the Lanbandeng granitoid intrusion and is hosted mainly by a diopside skarn that formed by high-temperature metasomatic exchange between the biotite granite and the adjacent Middle Devonian psammitic limestone. The mineralized diopside skarns and unmineralized skarns are concentrated in the outer contact zone of the biotite granite, but skarn minerals also occur within xenoliths of country rock in the inner contact zone (Li S Q et al., 2010).

The Wangjiaping granite is concealed and has an intrusive contact with the surrounding rock. The W-Mo ore is distributed mainly within the concealed intrusion, the outer contact zone, and the overlying country rock (Figs. 4, 6), and the ore distribution is structurally controlled. NNE–SSW-striking fractures are visible at the surface to the east and west of the concealed granite. These fractures radiate outwards from the granite contact (Fig. 6). The wall rock is silicified and skarnitized (Figs. 6, 7c, e, f, i), and the concealed inner granite contact zone is pervasively greisenized (Fig. 7b). The Mo mineralization is dominated by sparsely disseminated and fracture-filling molybdenite, and weak W mineralization (Fig. 7h). Within 140 m of the concealed granite margin, mineralization consists mainly of disseminated molybdenite, fine-grained mineralized granite veins, and rare W mineralization (Fig. 7a). In the country rock, at concealed granite margin of >300 m, the scheelite occurs

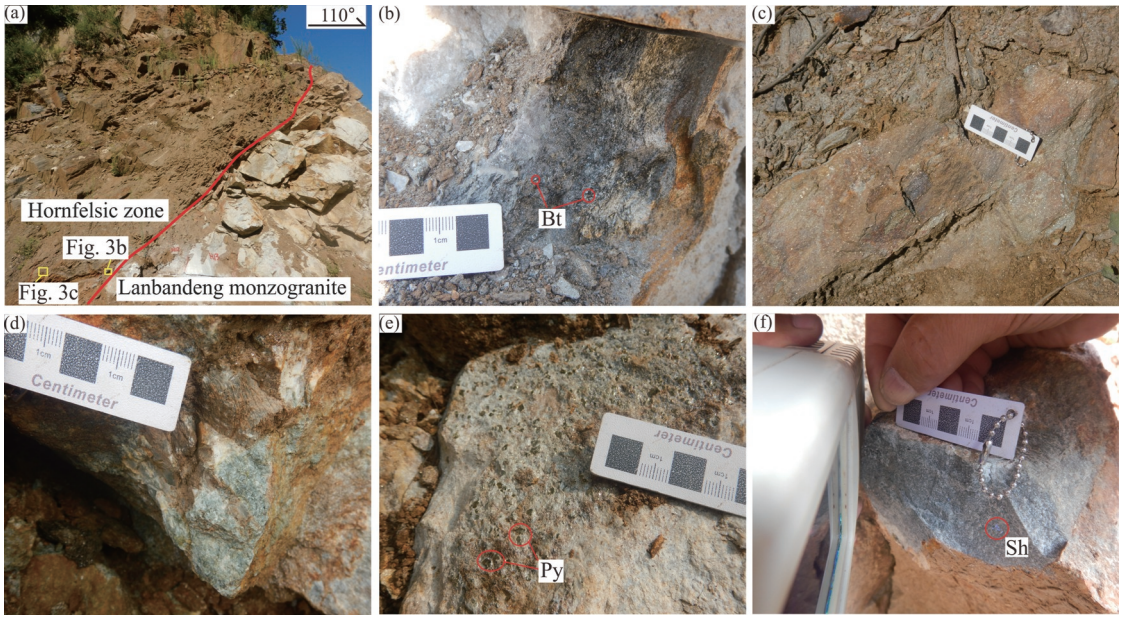

Fig. 3. Alteration and mineralization within the country rock of the Lanbandeng granitoid intrusion.
(a) Hornfelsic zone in northwest Lanbandeng granitoid intrusion; (b) Biotite hornization; (c) Limonitized biotite hornfels; (d) Skarnization in northeast Lanbandeng granitoid intrusion; (e) Pyrite-bearing skarn; (f) Tungsten-bearing skarnalized marble. Sh, scheelite; Bt, biotite; Py, pyrite.

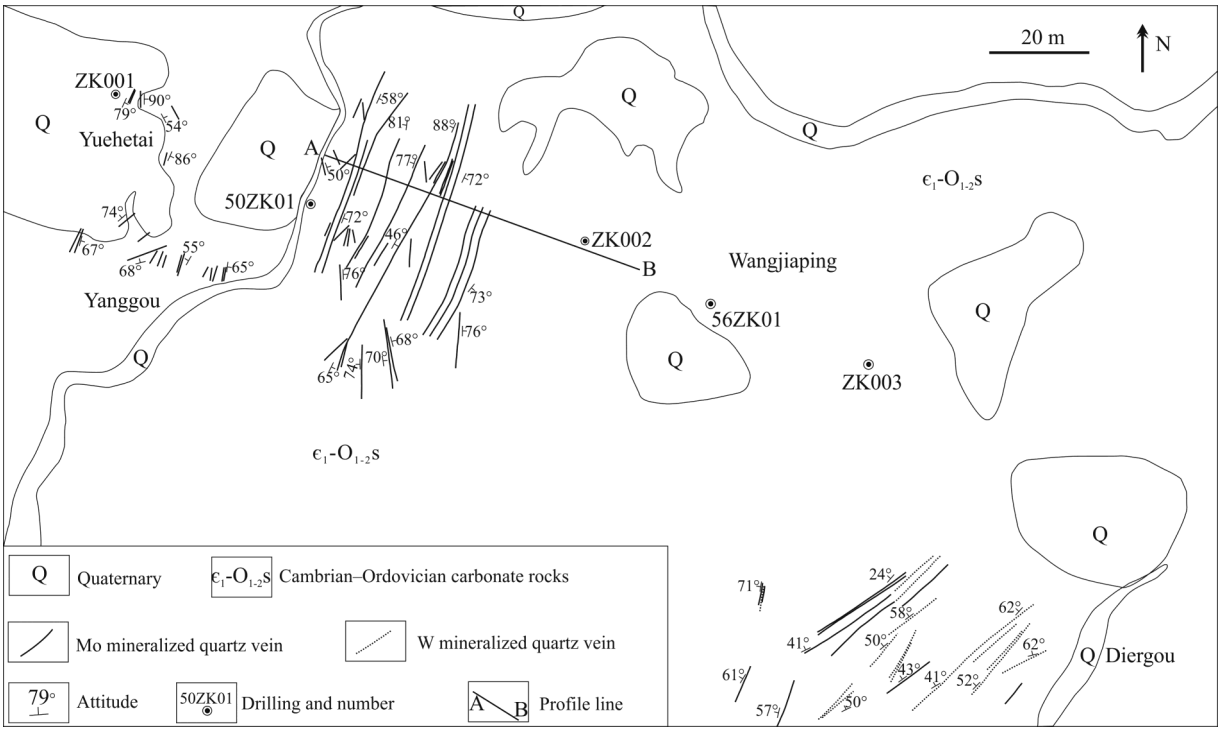

Fig. 4. Geological sketch of W-Mo mineralization associated with the Wangjiaping granite, modified after unpublished data (Shaanxi Mineral Resources and Geological Survey, 2018).

mainly within skarnitized marble within the outer contact zone and fracture-controlled quartz veins. Molybdenite is rare in this zone, but it occurs within quartz-feldspar pegmatite veins that cut the concealed intrusion (Fig. 7d, g). In summary, the W-Mo mineralization is spatially associated with the concealed granite and vertically zoned, comprising deep proximal Mo-mineralization and shallow distal W-mineralization (Zhou et al., 2016).

W-Mo ore bodies associated with quartz veins strike approximately N–S and NNE–SSW, and are 43–570 m long with a thickness of 0.46–1.09 m. In these units, the W grade is 0.72%–1.09%. The ore body is controlled mainly by (N)NE–(S)SW-trending faults and joints, and some E–W-trending faults (Figs. 4, 5). There are no obvious

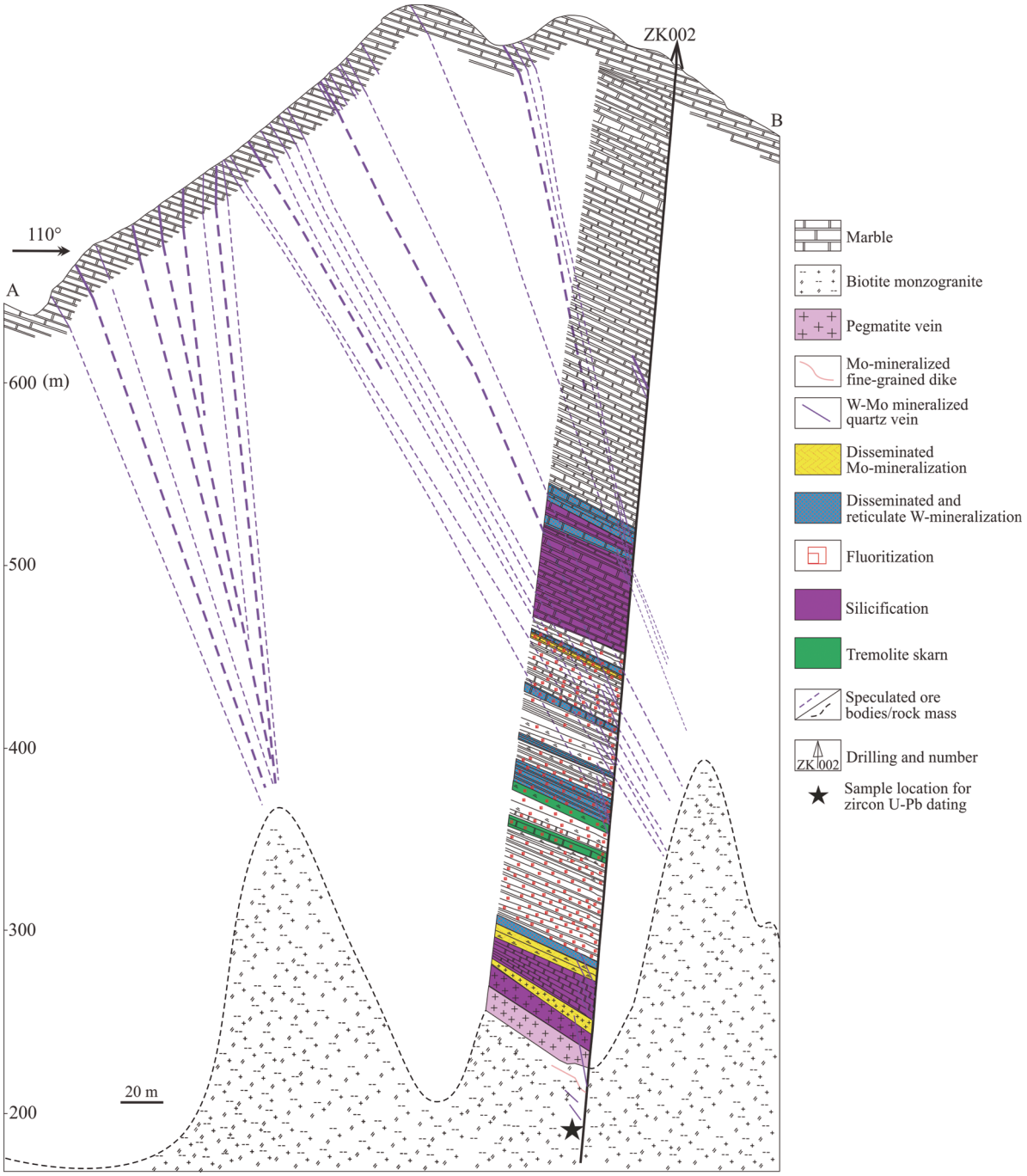

Fig. 5. Geological cross-section (A–B) showing alteration and mineralization at Wangjiaping.

crosscutting relationships between the N–S- or (N)NE–(S)SW-trending orebodies and the WNW–ESE-trending orebodies, so all the orebodies might have formed at the same time from hydrothermal fluids that infiltrated an orthogonal set of fractures. Quartz-vein-hosted mineralization occurs within the fractures and at the margins of quartz veins, and consists of scheelite, pyrite, and molybdenite (Fig. 8a–f). Skarn-type W-Mo mineralization occurs in the host rock of the intermediate–felsic intrusions, most commonly in Paleozoic limestones, dolomites, and marbles. Marble-veined-limestone, marbles, and skarns are common and crop out across scales of several to tens of meters. Skarn units are predominantly calcareous, magnesium, diaphanite, pyrite-garnet, epidote, epidote-diopside, and muscovite-epidote-diopside skarns. There are also dozens of stratiform skarn belts in the ore-bearing region, which are 100–1000 m long and 20–120 m wide. The W-Mo deposits associated with these belts are 900–1300 m long and 1.97–5.10 m thick, and are concentrated along fracture zones oriented WNW–ESE and NNE–SSW. The W grade in these skarn units is 0.42%–1.16%. The skarn assemblages comprise

Fig. 6. Features of the concealed intrusive body and associated alteration and mineralization in drill hole ZK002.
(a) Disseminated molybdenite within fine-grained granite; (b) Greisenized inner contact zone; (c) Skarnitized marble; (d) Feldspar-quartz pegmatite dyke cutting granite; (e) Silicified marble; (f) Secondary fluorite and chlorite in the country rock; (g) Molybdenite-bearing pegmatite; (h) Fractured quartz-molybdenite vein; (i) Tremolite skarn.. Qtz, quartz; Fs, feldspar; Mot, molybdenite; Fl, fluorite; Chl, chlorite.

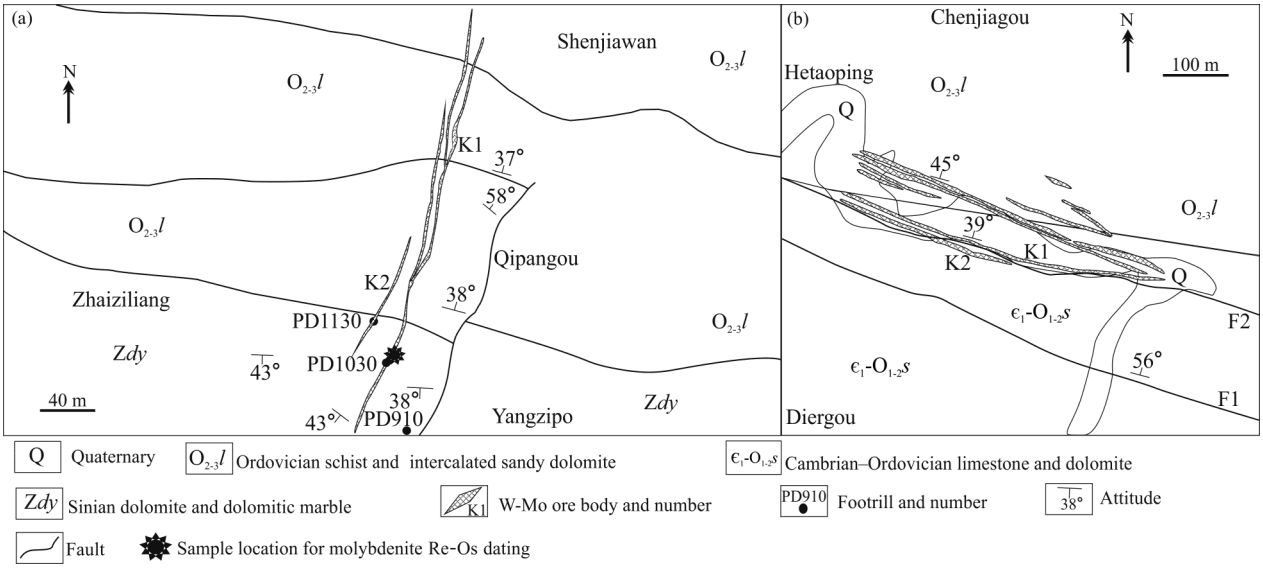

Fig. 7. Geological sketches of W-Mo mineralization at (a) Qipangou, modified after Ruan et al. (2019); and (b) Hetaoping, modified after Dai et al. (2019).

wollastonite, diopside, tremolite, garnet, muscovite, biotite, phlogopite, and beryl. W-Mo and Pb-Zn ores have also been identified in some skarn units (Fig. 8g–i). The residual-type W-Mo ore occurs mainly within the Dongyang deposit, with an endowment of 900,000 tons at an average W grade of 1.27%.

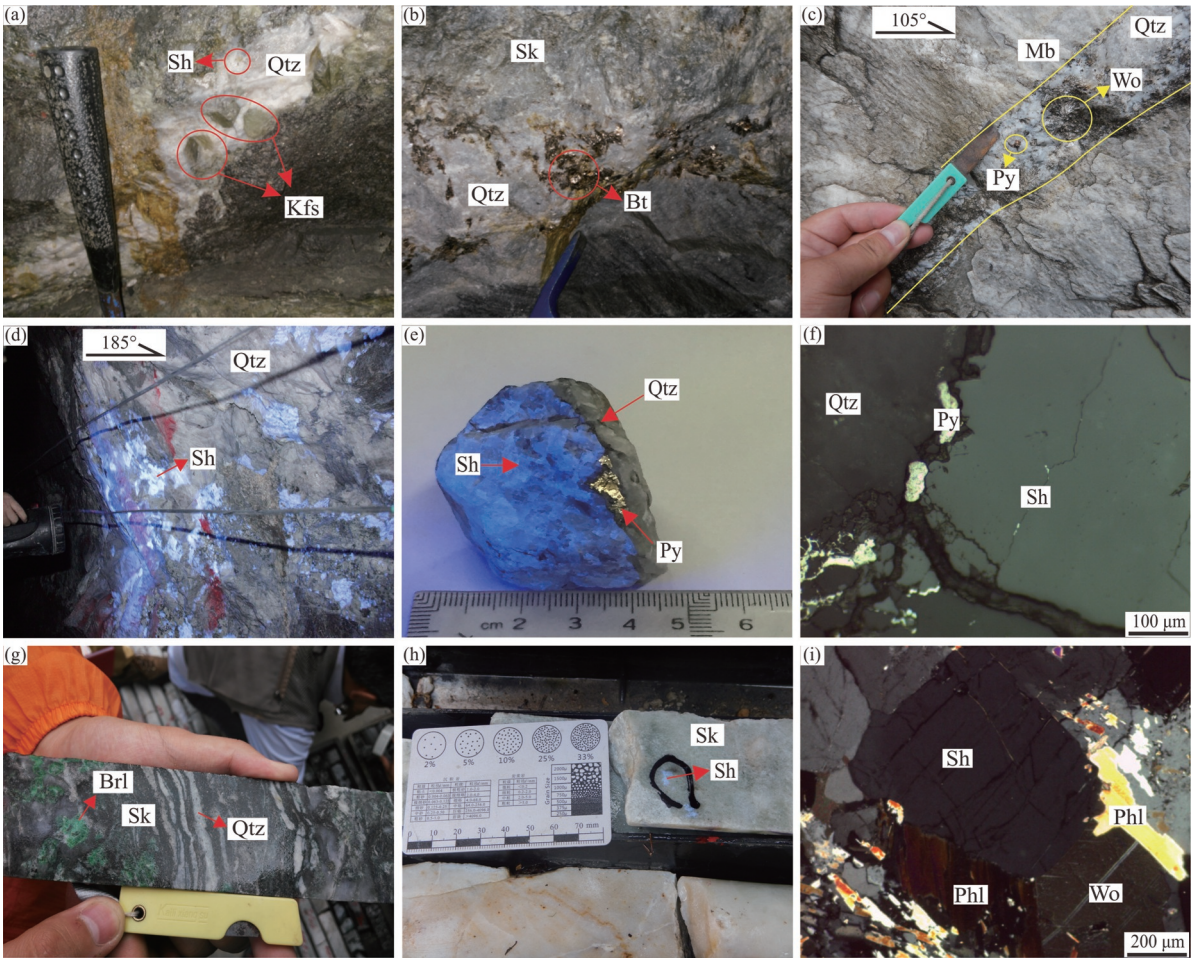

Fig. 8. Characteristics of W-Mo alteration and mineralization associated with the Qipangou and Hetaoping intrusions.
(a) Scheelite-bearing quartz-K-feldspar vein, Qipangou; (b) Biotite alteration in skarn, Qipangou; (c) Quartz vein containing wollastonite and pyrite, Qipangou; (d) Scheelite-bearing quartz vein from the footrill 1030, Qipangou; (e) Quartz-vein-type scheelite ore, Qipangou; (f) Photomicrograph of quartz-vein-type scheelite ore (XPL), Qipangou; (g) Beryl skarn, Hetaoping; (h) Scheelite-bearing skarn, Hetaoping; (i) Photomicrograph of scheelite-bearing skarn, Hetaoping; Abbreviations: Sh: scheelite; Qtz: quartz; Kfs: K-feldspar; Bt: biotite; Wo: wollastonite; Py: pyrite; Brl: beryl; Phl: phlogopite; Mb: marble; Sk: skarn; XPL: cross-polarized light.

4 Samples and Analytical Methods

4.1 Samples

The Lanbandeng monzogranite from the western Dongyang W-Mo deposit (sample Z1) and Wangjiaping biotite monzogranite from a drill core from the southwestern Hetaoping scheelite deposit (sample Z2) were sampled for U-Pb zircon geochronology. Sample Z1 is grayish white with a moderately coarse to fine granitic texture and massive structure. The main mineral constituents of Z1 are quartz (25%±), plagioclase (15–30%), and K-feldspar (40%–55%), with minor biotite (5%±) and muscovite (3%±) (Fig. 9a, d). Sample Z2 was taken from a depth of 552 m in core ZK002. It is grayish white and weakly chloritized, has a moderately coarse to fine granitic texture, and a massive structure. The main mineral phases are K-feldspar (45%), plagioclase (30%–45%), quartz (20%–25%), biotite (3%–5%), and chlorite (1%–2%). Sample Z2 also contains variably wide (several millimeters to tens of centimeters) quartz veins, disseminated molybdenite, and coarse localized pyrite aggregates (Fig. 9b, e).

A molybdenite-bearing sample was extracted from the footrill 1030 of the Qipangou quartz-vein-type W-Mo deposit for Re-Os geochronology (sample R1). Sample R1 contains both scheelite and molybdenite (Fig. 9c, f).

4.2 Analytical methods

4.2.1 U-Pb zircon geochronology

Zircons were separated at the Institute of Regional Geology and Mineral Resources Research, Hebei Province, China. Zircon preparation and cathodoluminescence (CL) imaging was conducted at the State Key Laboratory of Continental Dynamics, Northwest University, Shaanxi Province, China. Laser ablation inductively coupled plasma mass spectrometry (LA-ICP-MS) analyses for U-Pb zircon geochronology were completed at the Key Laboratory of West Mineral Resources and Geology Engineering Ministry of Education, Chang'an University, Shaanxi Province, China, using an Agilent 7700X quadrupole mass spectrometer coupled to an excelsior Photo Machines 193 nm laser. The

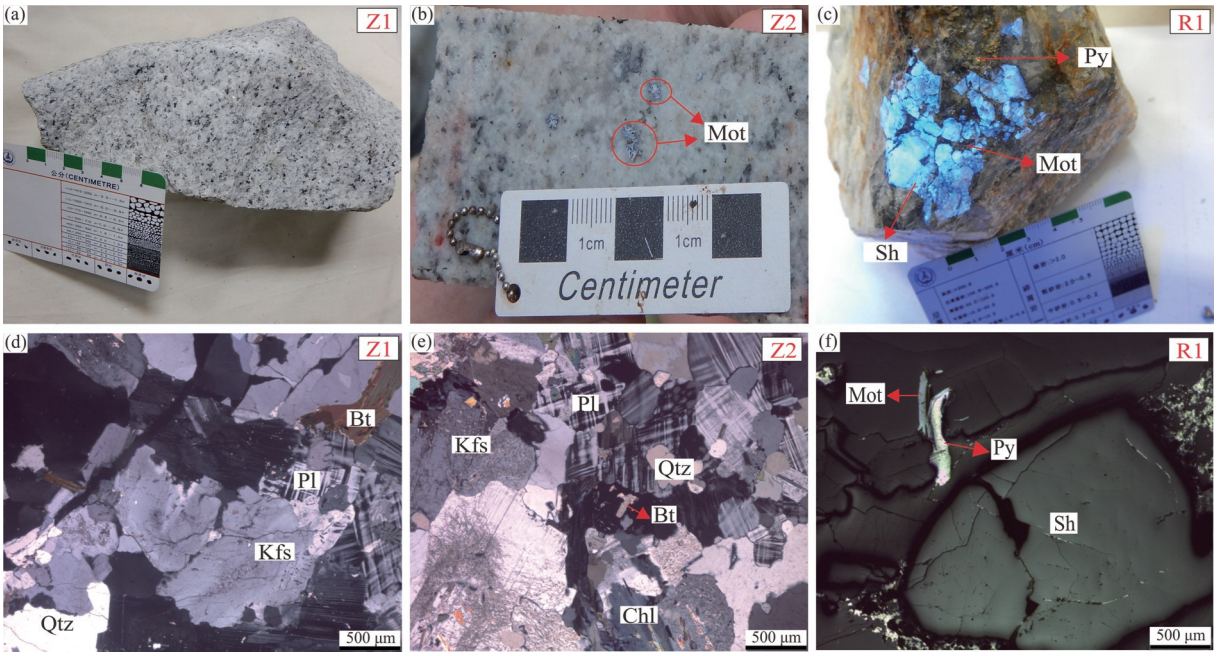

Fig. 9. (a) Hand specimen of Lanbandeng monzogranite; (b) Wangjiaping biotite monzogranite in drill core; (c) quartz-vein -type scheelite ore containing pyrite and molybdenite, Qipangou; (d) Photomicrograph of the Lanbandeng monzogranite (XPL); (e) photomicrograph of the Wangjiaping biotite monzogranite (XPL); (f) photomicrograph of quartz-vein-type scheelite ore, Qipangou (XPL).
Sh, scheelite; Qtz, quartz; Kfs, K-feldspar; Pl, plagioclase; Bt, biotite; Chl, chlorite; Py, pyrite; Mot, molybdenite.

laser beam spot had a diameter of 35 μm, a frequency of 5 Hz, an energy density of 5.9 J/cm^2, and collection time of 40 s. After every 6–8 points, the system was restandardized to NIST SRM610 and two 91500 zircon standards, and between each point a gas background was collected for 10 s. The washout time was 20 s. ICP-MS DataCal was used for offline data processing, and Isoplot v3.7 was used to calculate zircon weighted-mean ages and plot concordia diagrams. Further details of the experimental procedures and data analysis can be found in Gong et al. (2009a, b).

4.2.2 Re-Os molybdenite dating

Molybdenite separation was undertaken at the Institute of Regional Geology and Mineral Resources Research, Hebei Province, China. At least 500 mg of pure molybdenite was isolated for analysis, and Re-Os isotopic analyses were completed at the Key Re-Os Laboratory of China, Chinese Academy of Geological Sciences, Beijing, China. Powders were loaded into Carius tubes together with ^{185}Re and ^{190}Os spikes and were digested by reverse aqua regia at 230°C for ca. 24 h. Osmium was separated using distillation and microdistillation, and Re was extracted from the residue using acetone in a 8-M NaOH solution. The detailed analytical procedure is available in Li et al. (2009) and Li C et al. (2010). Both Re-Os concentrations and isotopic compositions were measured using a Thermo Fisher Scientific Triton Plus mass spectrometer operating in negative ion detection mode (Li C et al., 2015). Instrumental mass fractionation of Os was corrected by normalizing the measured ^{192}Os/^{188}Os ratio to 3.08271 (Nier, 1937). Based on blank runs analyzed together with samples, the total procedural blanks were ca. 3 pg for Re and 0.5 pg for Os. In-house sulfide Re-Os isotope reference JCBY from the Jinchuan Cu-Ni deposit was used for quality control.

5 Results

5.1 U-Pb zircon geochronology

Results of U-Pb zircon geochronology on the Lanbandeng monzogranite (sample Z1) and Wangjiaping biotite monzogranite (sample Z2) are presented in Table 1 and Fig. 10.

Zircons in sample Z1 range from colorless to yellowish and transparent. Most zircons are large and idiomorphic, although some are small and round. CL images document minor corrosion at zircon rims, but zoning is largely concentric and oscillatory and thus reflects primary magmatic growth zoning (Fig. 10a). All 12 analyses were concordant, indicating the U-Pb isotopic system remained closed during late metamorphism. The measured points intersect the concordia at 222.7 ± 2.6 Ma (MSWD = 0.33), with a weighted-mean of 222.7 ± 2.3 Ma (MSWD = 1.3) (Fig. 11a).

Zircons in sample Z2 are colorless and transparent, idiomorphic, and smaller than zircons of Z1. CL images reveal oscillatory magmatic growth zoning (Fig. 10b). Fourteen analyses are concordant, and the measured points intersect the concordia at an age of 201.6 ± 4.7 Ma (MSWD = 0.39), with a weighted-mean age of 201.9 ± 1.8 Ma (MSWD = 0.39). This age is slightly younger than sample Z1 (Fig. 11b).

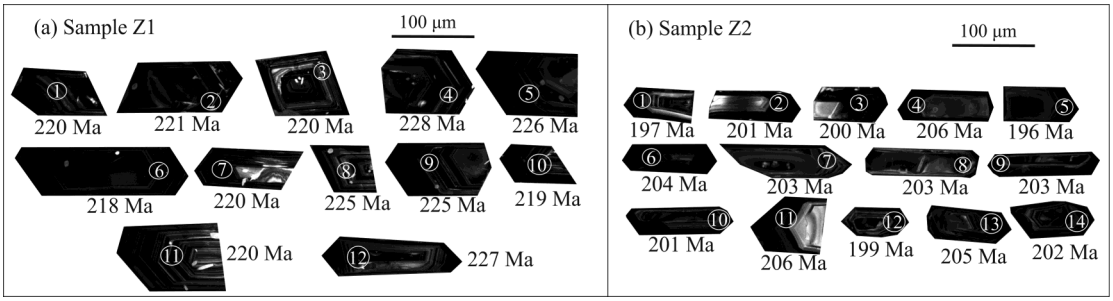

Fig. 10. Cathodoluminescence (CL) images of zircons from the (a) Lanbandeng monzogranite and (b) Wangjiaping biotite monzogranite from the W-Mo mineralized area.

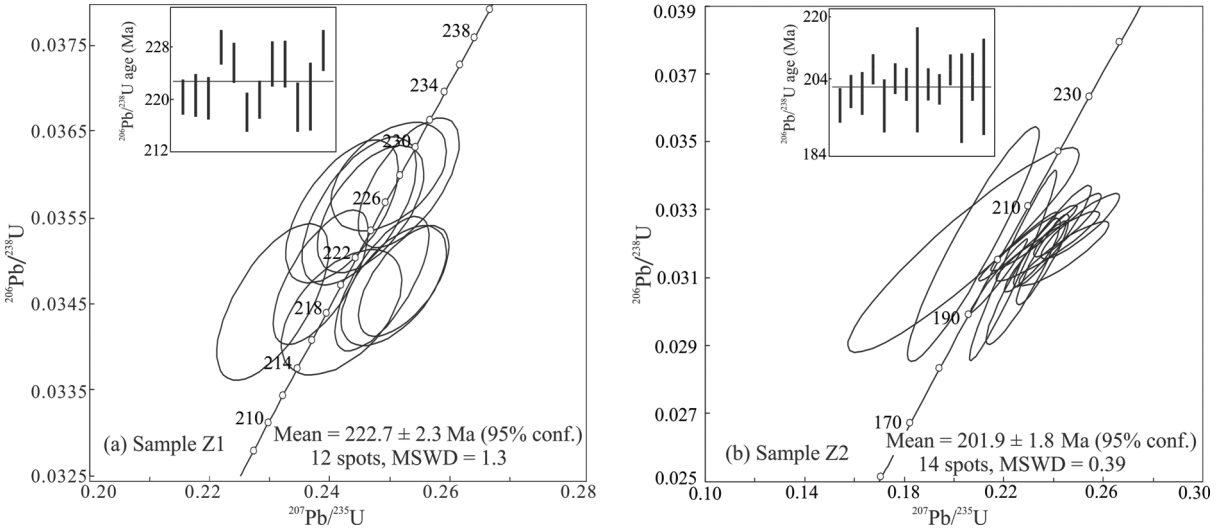

Fig. 11. U-Pb concordia plots for the (a) Lanbandeng monzogranite and (b) Wangjiaping biotite monzogranite from the W-Mo mineralized area.

Table 1 Zircon U-Pb age data for the Lanbandeng monzogranite (Z1) and Wangjiaping biotite monzogranite (Z2) from the W-Mo mineralized area

Spot	Element (ppm)			Th/U	Measured isotope ratio						Apparent age (Ma)					
	Pb	Th	U		$^{207}Pb/^{206}Pb$	1σ	$^{207}Pb/^{235}U$	1σ	$^{206}Pb/^{238}U$	1σ	$^{207}Pb/^{206}Pb$	1σ	$^{207}Pb/^{235}U$	1σ	$^{206}Pb/^{238}U$	1σ
Sample Z1 (monzogranite)																
1	151	1720	3783	0.45	0.05249	0.00109	0.25235	0.00498	0.03477	0.00043	306	48	228	4	220	3
2	104	1774	2475	0.68	0.04954	0.00103	0.23846	0.00523	0.03481	0.00052	172	48	217	4	221	3
3	181	2714	4417	0.60	0.05173	0.00100	0.24875	0.00520	0.03474	0.00052	272	44	226	4	220	3
4	109	1605	2618	0.61	0.05000	0.00121	0.24982	0.00635	0.03599	0.00042	195	25	226	5	228	3
5	133	1375	3382	0.41	0.05003	0.00109	0.24684	0.00584	0.03561	0.00049	195	55	224	5	226	3
6	86	1299	2121	0.60	0.05084	0.00137	0.24199	0.00663	0.03441	0.00048	235	63	220	5	218	3
7	130	2063	3149	0.65	0.05221	0.00117	0.25070	0.00576	0.03471	0.00046	295	52	227	5	220	3
8	93	1108	2314	0.47	0.04921	0.00125	0.24205	0.00621	0.03558	0.00055	167	59	220	5	225	3
9	115	2072	2694	0.77	0.04856	0.00168	0.24492	0.00633	0.03558	0.00057	128	81	222	5	225	4
10	98	1556	2425	0.63	0.04631	0.00227	0.23049	0.00612	0.03453	0.00060	13	115	211	5	219	4
11	134	2141	3244	0.65	0.04979	0.00161	0.24627	0.00588	0.03478	0.00083	183	74	224	5	220	5
12	121	1853	2856	0.63	0.05099	0.00107	0.25315	0.00554	0.03591	0.00050	239	48	229	4	227	3
Sample Z2 (biotite monzogranite)																
1	63	694	1278	0.52	0.04755	0.00291	0.21804	0.00760	0.03105	0.00071	76	80	200	6	197	4
2	55	425	1573	0.25	0.05194	0.00291	0.23276	0.00819	0.03162	0.00069	283	80	212	7	201	4
3	109	705	3640	0.20	0.12724	0.07850	0.23565	0.00701	0.03154	0.00088	2061	67	215	6	200	6
4	48	315	1549	0.18	0.05444	0.00180	0.24568	0.00897	0.03254	0.00062	391	69	223	7	206	4
5	53	592	941	0.54	0.06725	0.01718	0.22770	0.00986	0.03090	0.00122	856	99	208	8	196	8
6	46	496	1045	0.42	0.05302	0.00312	0.23221	0.01150	0.03216	0.00064	328	109	212	9	204	4
7	23	215	520	0.35	0.05424	0.00332	0.23758	0.01362	0.03192	0.00067	389	122	216	11	203	4
8	34	359	597	0.42	0.04015	0.00509	0.20768	0.01738	0.03199	0.00229	408	127	192	15	203	14
9	48	452	1139	0.35	0.05165	0.00282	0.22563	0.01047	0.03192	0.00066	333	124	207	9	203	4
10	68	794	1301	0.58	0.05588	0.00277	0.24399	0.01189	0.03171	0.00062	456	100	222	10	201	4
11	58	543	1512	0.34	0.05563	0.00205	0.25067	0.01051	0.03252	0.00064	439	81	227	9	206	4
12	80	638	1623	0.40	0.06639	0.02376	0.22369	0.01144	0.03135	0.00184	820	119	205	9	199	12
13	225	1483	6752	0.24	0.04781	0.00434	0.23949	0.01025	0.03223	0.00098	100	74	218	8	205	6
14	55	419	942	0.58	0.03498	0.00667	0.20394	0.03065	0.03182	0.00198	365	89	188	26	202	12

5.2 Re-Os molybdenite geochronology

The Re-Os molybdenite geochronological data yielded a model age of 199.7 ± 3.9 Ma (Table 2). The Qipangou W-Mo deposit therefore formed in the Early Jurassic, with metallogenesis occurring in the early Yanshanian.

6 Discussion

6.1 Crystallization age

Numerous studies have constrained the ages of granitoid intrusions in mineralized areas of South Qinling, China. These largely utilize single-grain U-Pb zircon geochronology by LA-ICP-MS or sensitive high-resolution ion microprobe (SHRIMP) techniques, and the results of these studies and our data are summarized in Table 3 and Fig. 12.

There are extensive age data for the Dongjiangkou and Yanzhiba composite granite bodies, whereas the Lanbandeng and Sihaiping granitic intrusions are relatively poorly constrained in terms of age. Late Triassic to Early Jurassic granitoid intrusions in the mineralized area have ages of 240–190 Ma, with a peak at 220–210 Ma, and a final stage of magmatic activity at 200–190 Ma (Fig. 12). The four main granitoid intrusions are composite intrusions, and the protracted Late Triassic to Early Jurassic history recorded by the dated rocks are consistent with a multi-stage intrusive model (Fig. 12). Multiple mineralization episodes are likely to have occurred, and some intrusions may have served as mineralization precursors (e.g., the Wangjiaping biotite monzogranite).

Evidence for multiple episodes of granitic magmatism and W mineralization is commonplace. Studies of W deposits in South China have documented two or more episodes of Yanshanian granite intrusion associated with quartz vein- and skarn-type W-Mo deposits, but most of the mineralization is associated with a single episode. These intrusions are likely the result of numerous magma

Table 2 Re-Os geochronological data for the Qipangou W-Mo deposit.

Sample	Weight (g)	Re (ng/g)		Common Os (ng/g)		^{187}Re (ng/g)		^{187}Os (ng/g)		Model age (Ma)	
		Measured	2σ	Measured	2σ	Measured	2σ	Measured	2σ	Measured	2σ
R1	0.00531	187630	1191	3.181	0.355	117929	749	393.0	6.1	199.7	3.9

Table 3 Compiled geochronological results from major intrusions in the W-Mo mineralized areas.

Granitoid pluton	Rock	Mineral	Analysis method	Age (Ma)	Reference
Dongjiangkou	Monzogranite	Zircon	LA-ICP-MS U-Pb	209 ± 2 219 ± 2	Yang et al., 2009
	Granodiorite	Biotite	Ar-Ar	198	Zhang et al., 2006
	Porphyritic granodiorite	Zircon	LA-ICP-MS U-Pb	219 ± 2	Liu et al., 2011
	Monzogranite	Zircon	SHRIMP U-Pb	211 ± 3	Liu et al., 2011
	Quartz monzonite	Zircon	U-Pb	211 ± 2	Sun et al., 2000
	Monzogranite	Zircon	U-Pb	199 ± 12	Zhang et al., 2006
	Tonalite	Zircon	LA-ICP-MS U-Pb	220 ± 2	Qin, 2010
	Mafic enclaves	Zircon	LA-ICP-MS U-Pb	219 ± 2	Qin, 2010
	Granodiorite	Zircon	LA-ICP-MS U-Pb	214 ± 2	Qin, 2010
	Granodiorite	Zircon	LA-ICP-MS U-Pb	222 ± 2	Qin, 2010
	Mafic dikes	Zircon	LA-ICP-MS U-Pb	216 ± 2	Qin, 2010
	Granite	Zircon	LA-ICP-MS U-Pb	222.6 ± 0.5	Gong et al., 2009a
	Mafic enclaves	Zircon	LA-ICP-MS U-Pb	221.6 ± 0.6	Gong et al., 2009a
	Mafic enclaves	Zircon	LA-ICP-MS U-Pb	222.0 ± 0.5	Gong et al., 2009a
	Monzogranite	Zircon	LA-ICP-MS U-Pb	218 ± 3	Ping et al., 2013
	Granite	Zircon	SHRIMP U-Pb	218.7 ± 2.4	Jiang et al., 2010
Yanzhiba	Biotite granite	Zircon	LA-ICP-MS U-Pb	201.9 ± 1.5	Wei et al, 2016
	Biotite granite	Zircon	LA-ICP-MS U-Pb	201.6 ± 1.2	Dong et al., 2012
	Monzogranite	Zircon	SHRIMP U-Pb	210.8 ± 5	Jiang et al., 2010
	Monzogranite	Zircon	LA-ICP-MS U-Pb	214	Zhang et al., 2001
	Dimica monzogranite	Zircon	LA-ICP-MS U-Pb	208 ± 2 209 ± 2	Liu et al., 2011
	Monzogranite	Zircon	LA-ICP-MS U-Pb	222±1	Liu et al., 2011
	Biotite granite	Zircon	LA-ICP-MS U-Pb	200 ± 4	Luo, 2010
	Monzogranite	Biotite	^{40}Ar-^{39}Ar	185 ± 1	Zhang et al., 2006
Sihaiping	Granite	Zircon	LA-ICP-MS U-Pb	199 ± 1. 4	Zhang et al., 2015
	Moyite	Zircon	LA-ICP-MS U-Pb	201 ± 3.1	Zhang et al., 2015
	Porphyritic granite	Zircon	LA-ICP-MS U-Pb	198 ± 11	Zhang et al., 2015
	Biotite monzogranite	Zircon	LA-ICP-MS U-Pb	168.2 ± 1.1	Chen et al., 2017
Lanbandeng	Biotite granite	Zircon	LA-ICP-MS U-Pb	200 ± 1.9	Liu et al., 2013
	Biotite monzogranite	Zircon	LA-ICP-MS U-Pb	222.7 ± 2.3	This study
	Monzogranite	Zircon	LA-ICP-MS U-Pb	209 ± 2	Yang et al.2011
Wangjiaping	Biotite monzogranite	Zircon	LA-ICP-MS U-Pb	201.9 ± 1.8	This study

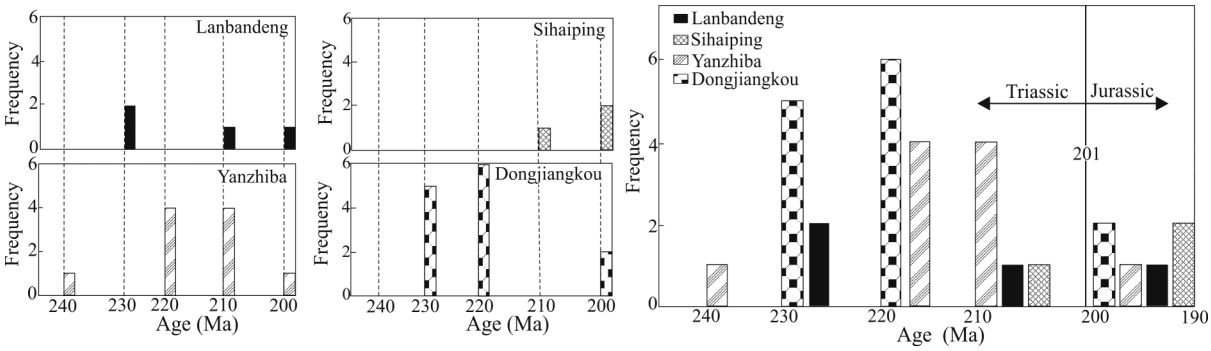

Fig. 12. Age histogram for granitoid intrusions in the mineralized area.

Table 4 Summary of ages of W-Mo deposits in the mineralized area.

Deposit	Mineralization type	Mineral	Method	Age (Ma)	Reference
Xinpu	Quartz vein-type Mo deposit	Molybdenite	Re-Os	197.0 ± 1.6	Dai et al., 2015
Dongyang	Skarn-type W-Mo deposit	Molybdenite	Re-Os	198 ± 2.7	Liu, 2013
Hetaoping	Skarn-type W-Mo deposit	Molybdenite	Re-Os	196.3 ± 3.3	Dai et al., 2018
Yueheping	Skarn-type Mo deposit	Molybdenite	Re-Os	194 ± 4	Li, et al., 2010a
Guilingou	Biotite granite- and quartz vein-type Mo deposit	Molybdenite	Re-Os	197.2 ± 1.3	Zhang et al., 2015
Qipangou	Quartz vein-type W-Mo deposit	Molybdenite	Re-Os	199.7 ± 3.9	This study
Jiangkou	Quartz vein-type Mo deposit	Molybdenite	Re-Os	198.7 ± 3.9	Unpublished data

fluxes during the same orogenic episode, with temperature and pressure changes, volatile components are progressively depleted and the crystallizing mineral compositions changed and precipitated in different host rock settings. As a consequence, a variety of interpenetrating mineral veins formed. Fluid compositions are also likely to have varied during crystallization, resulting in the development of reverse zoning in the granitic bodies, with W-Sn minerals towards the top and sulfide minerals towards basal levels. Thus, multiple horizons of W mineralization resulted from these cyclical episodes of granitic magmatism (Kang, 1959).

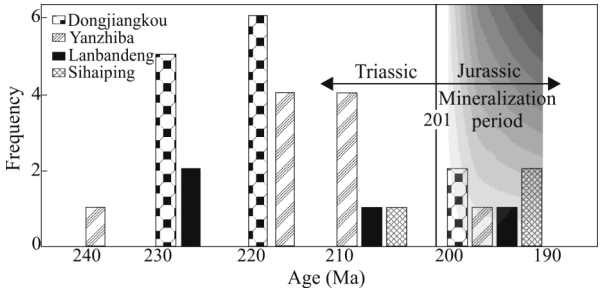

Fig. 13. Comparison of granitoid and W-Mo mineralization ages in the mineralized area.

6.2 Metallogenic age and source of the ore-forming material

The beta decay system of ^{187}Re decays to ^{187}Os can be utilized to determine the age of molybdenite crystallization (Mc Candless et al., 1993). As a consequence of its relatively high closure temperature (500–600°C; Rollinson, 1993), the Re-Os system is not susceptible to alteration by late tectonic or hydrothermal activity, and so the measured age generally represents the age of mineralization (Stein et al., 2001). The close association of scheelite and molybdenite in the mineralized area reflects their contemporaneous mineralization, meaning that Re-Os molybdenite geochronology can also be used to determine the age of scheelite crystallization.

Re-Os molybdenite ages generally fall within the Early Jurassic at 200–190 Ma (Table 4; Fig. 13). These ages are at odds with the timing of the three other major Mo metallogenic periods in Qinling, which were at 238–213 Ma, 145–126 Ma, and 116–110 Ma (Mao et al., 2009b; Li et al., 2012). The age of W-Mo mineralization in the mineralized area determined in this study is later than the first metallogenic period along the southern margin of the North China Block and North Qinling tectonic belt (238–213 Ma), and earlier than the second metallogenic period (145–126 Ma). Therefore, our reported metallogenic ages may represent a stage of W-Mo mineralization in the South Qinling metallogenic belt that has not yet been recognized.

Granitoids in the study region have ages (210–220 Ma) that are 10–20 Myr older than those of the W–Mo mineralization. However, the timing of later magmatic activity (200–190 Ma) coincides with the age of mineralization, and magmatism is therefore interpreted to be the thermal driver of mineralization. Magmatic bodies may have also acted as an additional source of ore-forming components that facilitated mineralization.

The Wangjiaping biotite monzogranite has an age of 201.9 ± 1.8 Ma, within the transitional period from the Triassic to Jurassic, and similar to Re-Os ages (200–196 Ma) of molybdenite in the mineralized area. Drill cores show that fine-grained granitic veins associated with molybdenite are present both at intermediate and shallow levels of the biotite monzogranite. W-Mo mineralization is also present in skarn marble and quartz vein fissures near

the periphery of the granite body, and there is a preference for systematic upper scheelite and lower molybdenite vertical cyclic enrichment. The Wangjiaping granite is peraluminous and calc-alkaline with high Si, low Ti and P, and $(La/Yb)_N \approx 1$. The bulk composition is strongly depleted in Eu, and the rare earth element chondrite-normalized plot shows either slight enrichment in light rare earth elements relative to heavy rare earth elements, or is near-flat with a central dip. These characteristics are similar to mineralized granites in South China, which are more suited to W mineralization (Zhou et al., 2016). The igneous rocks associated with W-Mo mineralization in South China are mainly medium–small intermediate–felsic complex intrusions, with granitic and medium–fine-grained biotite granitic lithologies (Bi, 1987). Based on studies of the Gaojiabang W-Mo deposit in Qingyang, Anhui Province, Xiao et al. (2017) suggested that highly fractionated S-type granites, and aluminous to weakly aluminous granites consisting of a mixture of crustal and mantle components, are favorable for W-Mo mineralization. A biotite granite with a zircon U-Pb age of 200 ± 4 Ma in the Yanzhiba composite granite body is Si- and alkali-rich, and belongs to the high-K calc-alkaline series (Luo et al., 2010). The evidence indicates that the intermediate–felsic Wangjiaping biotite monzogranite that formed at 200–190 Ma is genetically linked to W-Mo mineralization in the mineralized area.

Re is rarely present in high concentrations in natural minerals. Molybdenite is the main carrier of Re and provides >80% of global Re supply. Studies have shown that the Re content of molybdenite may be used to trace the source of ore-forming materials and constrain the degree of source mixing during mineralization (Mao et al., 1999a; Stein et al., 2001; Sun et al., 2015). Mao et al. (1999a) analyzed the Re content of molybdenite in a range of Mo deposits in China, and determined that Re concentrations in ores decrease by orders of magnitude depending on the source, a result also confirmed by subsequent researchers (Li et al., 2003, 2006; Ye et al., 2006; Li et al., 2007; Zhang et al., 2009). The Re concentration of molybdenite derived from mantle sources is ca. 100–1000 μg/g (Huang, 1994; Hou et al., 2003; Meng et al., 2003), crustally derived molybdenite deposits generally have Re < 10 μg/g (Li et al., 1996; Mao et al., 1999b), and Re concentrations in molybdenite derived from mixed crust-mantle sources is intermediate between these values (Huang et al., 1996; Feng et al., 2009). While Re contents clearly reflect the source of material, there is no systematic explanation for this variability.

The Re contents of molybdenite in the W-Mo mineralized area are 1.98–192.98 ppm (Table 5), with an average of 95.35 ppm. Therefore, the deposit was likely derived from a mixed crustal and mantle source, consistent with the mixed geochemical characteristics of the late Yanzhiba granite intrusion.

In situ LA-MC-ICP-MS scheelite data show that early oxide-stage scheelite from the Hetaoping deposit has an $^{87}Sr/^{86}Sr$ ratio of ~0.709. This value is close to the mantle value (0.704 ± 0.002), indicating that deep-sourced felsic magma might have provided the ore-forming elements for mineralization of the skarn stage to early oxide stage. In contrast, the $^{87}Sr/^{86}Sr$ ratios of late oxide-stage scheelite are 0.710–0.712, which are closer to crustal $^{87}Sr/^{86}Sr$ ratios (0.718 ± 0.02) than are the values of the early ore, but still significantly lower. The scheelite $^{87}Sr/^{86}Sr$ ratios are lower in the deep mineralization than in the shallow mineralization, consistent with extensive interaction and metasomatism between the ore-forming fluid and the country rock (Dai et al., 2019). The Sr isotope composition of early oxide scheelite at the Hetaoping W deposit is similar to that of intermediate–felsic igneous rocks (200–190 Ma) in the area. The $(^{87}Sr/^{86}Sr)_i$ value of the Lanbandeng biotite monzogranite (200 ± 1.9 Ma) at the Dongyang deposit is 0.7040–0.7068, the $^{143}Nd/^{144}Nd$ value is 0.512225–0.512326, and $\varepsilon_{Nd}(t) = -5.53$ to -4.28, reflecting the involvement of mantle enriched by crustal components or evolved from lithospheric mantle (Liu, 2013). The $(^{87}Sr/^{86}Sr)_i$ value of the Yanzhiba biotite granite (201.9 ± 1.5 Ma) is 0.70431–0.70678, and $\varepsilon_{Nd}(t) = -5.2$ to -2.0. The $(^{87}Sr/^{86}Sr)_i$ value and $\varepsilon_{Nd}(t)$ increase linearly with increasing SiO_2, consistent with assimilation of country rock during magma ascent. The similarity between the isotope characteristics of the granite and the initial Sr-Nd isotope composition of local Neoproterozoic volcanic sedimentary rocks (e.g., the Yaolinghe, Wudang, and Bikou groups) indicates that the dominant source of the Yanzhiba granite was Neoproterozoic crustal material with an affinity to the Yangtze Block (Wei et al., 2016). The Sr-Nd-Pb isotope ratios and the zircon Lu-Hf isotope composition indicate that the Yanzhiba biotite granitoids (~200 Ma) are partial melts of the middle crust that formed during lithospheric extension, with minor contributions from the lower crust or mantle-derived fluids (Qin, 2010). The initial Sr isotope composition of scheelite from the Hetaoping deposit is similar to that of the Lanbandeng and Yanzhiba granite bodies. This supports the notion that the 200–190 Ma granites were the main source of ore-forming elements (e.g., W, Mo, Sr) and that the widespread W(-Mo) mineralization within the Ningshan–Zhen'an area is closely related to intermediate–felsic magmatic-hydrothermal activity, which transported heat and ore-forming elements from the upper mantle and

Table 5 Re contents of molybdenite in the mineralized area

Deposit	Re (ppm)	Re source	Reference
Xinpu quartz vein-type Mo deposit	1.98–14.43	Crust	Dai et al., 2015
Dongyang skarn-type W-Mo deposit	151.34	Crust–mantle	Liu, 2013
Hetaoping skarn-type W-Mo deposit	85.32	Crust–mantle	Dai et al., 2018
Yueheping skarn-type Mo deposit	59.09–184.4	Crust–mantle	Li, et al., 2010a
Guilingou biotite granite- and quartz vein-type Mo deposit	92.29–192.98	Crust–mantle	Zhang et al., 2015
Qipangou quartz vein-type W-Mo deposit	187.63	Crust–mantle	This study
Jiangkou quartz vein-type Mo deposit	17.06	Crust–mantle	Unpublished data

lower crust to the shallow crust. Therefore, the transport and cycling of material between the crust and mantle favor the formation of W and Mo polymetallic deposits.

6.3 Intrusive and mineralization setting

W deposits are usually found in continental crust distal to subduction zones, and some are related to post-collisional fault structures and magmatism. In South China, W deposits predominantly formed during the early Yanshanian period (ca. 135–190 Ma), and the associated tectonic setting changed during orogenesis from fold- to fault-dominated deformation. In contrast, the Cenozoic has been dominated by extensional tectonics. As a consequence of this tectonic inversion, faulted settings in mature continental crust serve as the main site for the formation of W deposits in both South and East China (Xu and Cheng, 1987). Most W ore is found within intracontinental orogenic settings, where crustal-scale fault networks and widespread magmatism creates favorable conditions for the formation of superlarge W deposits (Sheng et al., 2015).

The South Qinling tectonic belt experienced intense intracontinental orogenesis in the Mesozoic and Cenozoic, and was an important tectonic unit during the development of the Qinling orogenic belt (Zhang et al., 1995, 2001, 2004). The long-term structure and orientation of the E–W -striking Qinling belt was controlled by Laurasia, the Paleo-Tethys Ocean, and the Gondwana Plate prior to the Mesozoic. During the Mesozoic and Cenozoic, N–S-striking structures formed in a transitional period while the Qinling belt was situated at the intersection between the Eurasian, Indian, and Pacific plates (Zhang et al., 2001, 2004; Zhu et al., 2008).

This change in paleo-tectonic setting yielded a new mantle dynamic system, and the direction of mantle flow direction in South Qinling changed to ~N–S (Zhang et al., 1995, 2001; Zhu et al., 2008), which caused lithospheric delamination and thinning and asthenospheric upwelling. Upwelling of the mantle and associated heat transfer led to crust-mantle material exchange, intrusive heating of the middle and lower crust, and thickening of the lower crust to form granitic magma, which ascended along weaknesses in the tectonic belt to form a large number of granites and related porphyry (skarn) deposits (Zhu et al., 2008, 2010; Mao et al., 2011b). Subsequent deformation and granitic magmatism, accompanied by large-scale mineralization, resulted in the development W-Mo-Au assemblages. This intracontinental orogenesis and the associated fluid processes resulted in the most important mineralization period in the South Qinling orogenic belt, enriching the region in Mo, Au, Hg, and Sb (Luo et al., 2007).

During the Late Triassic–Early Jurassic, the onset of collisional uplift in the Qinling orogenic belt resulted in the emplacement of numerous collisional granites, such as the Dongjiangkou, Zhashui, Caoping, and Shahewan granitic batholiths. As a consequence of the delay in timing of magmatism compared with subduction, the granite ages (200–190 Ma) are younger than the cessation of subduction, but share some characteristics with subduction-type granites (Li N et al, 2015), which have a transitional geochemistry between I- and A-type granites. This inference is also supported by the fact that these granites were derived from mixed crustal and mantle sources (Hu et al., 2004; Zhang et al., 2008; Gong et al., 2009a, b; Yang et al., 2009; Wang et al., 2011). As a consequence of these processes, related Mo deposits were formed, such as those at Yueheping, Guilingou, and Xinpu. The W-Mo mineralization formed during intracontinental orogenesis in the late Indosinian–Yanshanian, after the main Indosinian collisional period in the Qinling orogenic belt. The tectonic setting during intrusion and mineralization transitioned from compression to transtensional, and the South Qinling belt preserves a history of this transition. Intracontinental mineralization occurred during the magmatic-hydrothermal event that resulted from orogenic collapse after the main collision.

7 Conclusions

(1) The U-Pb zircon age of the Lanbandeng monzogranite is 222.7 ± 2.3 Ma. The U-Pb zircon age of the Wangjiaping biotite monzogranite is 201.9 ± 1.8 Ma. The Re-Os model age of molybdenite in the Qipangou W-Mo deposit is 199.7 ± 3.9 Ma, indicating that the W-Mo deposit formed during the Early Jurassic, in the Yanshanian period.

(2) Granitoid intrusions in the mineralized area are characterized by composite granite bodies. The ages of the granites are ca. 240–190 Ma, with peak magmatism at 220 –210 Ma, and waning activity at 200–190 Ma (i.e., the Wangjiaping biotite monzogranite). There are numerous episodes of activity within this period. Re-Os molybdenite ages are most commonly ca. 200–190 Ma, a time that may reflect a previously undiscovered stage of W-Mo mineralization in the South Qinling belt. The late magmatism at 200–190 Ma was most likely the driver of metallogenesis, and may also have provided an additional supply of ore-forming materials. The ore-forming materials in the W-Mo mineralized area were derived from mixed crustal and mantle sources.

(3) The W-Mo ore-region formed during intracontinental orogenesis in the Qinling orogenic belt during the late Indosinian–Yanshanian. During this time, the tectonic setting transitioned from compression to transtensional.

Acknowledgements

This research was co-funded by (1) Shaanxi Mineral Resources and Geological Survey (Grant no. 214027160195), a project on magmatism and W-Mo mineralization in the mineralized areas of western Zhen'an and (2) Shaanxi Mineral Resources and Geological Survey (Grant no. 61201506280), a project that combined exploration and technical approaches in the mineralized areas of the Qinling mineralized belt. We thank Mr. Liu Shaowu, general manager of the Dingfeng mining company, Zhen'an, Shaanxi Province, China, and Mr. Liu Xiangwei of the Shaanxi Mineral Resources and Geological Survey, China, for their valuable help and

support during field work.

Manuscript received Jun. 20, 2019
accepted Jan. 13, 2020
associate EIC: FEI Hongcai
edited by GUO Xianqing

Reference

Bi, C.S., 1987. Basic geological characteristics of skarn-type scheelite deposit in China. Bulletin of the Chinese Academy of Geological Sciences, 17(03): 49–64 (in Chinese with English abstract).

Chen, Q.M., Guo, Q.M., Wang, Q., Wang, Z., and Zhang, S.H., 2017. Zircon U-Pb dating and geochemical characteristics of Sihaiping pluton from Southern Qinling orogenic belt in Shaanxi. Northwestern Geology, 50(03): 65–73 (in Chinese with English abstract).

Dai, H.Z., Wang, D.H., Wang, C.H., and Huang, F., 2018. Re-Os isotopic dating of a W-Be polymetallic deposit, in the Southern Qinling region, China. Acta Geologica Sinica (English edition), 92(1): 414–415.

Dai, H.Z., Wang, D.H., Liu, L.J., Huang, F., and Wang, C.H., 2019. Metallogenic epoch and metallogenic model of the Hetaoping W-Be deposit in Zhen'an County, South Qinling. Acta Geologica Sinica, 93(6): 1343–1358 (in Chinese with English abstract).

Dai, J.Z., Yu, K.P., Wang, R.Y., Yuan, H.C., Wang, L., Zhang, X.S., and Li, J.B., 2015. Geological characteristics, Re-Os geochronology of Xinpu molybdenum deposit in Ningshan, southern Qinling and its implications. Acta Petrologica Sinica, 31(01): 189–199 (in Chinese with English abstract).

Dong, Y.P., Liu, X.M., Zhang, G.W., Chen, Q., Zhang, X.N., Li, W., and Yang, C., 2012. Triassic diorites and granitoids in the Foping area: Constraints on the conversion from subduction to collision in the Qinling Orogen, China. Journal of Asian Earth Sciences, 47(S1): 123–142.

Du, Y.L., Tang, Z.L., Cai, K.Q., Li, W.Y., and Zhang, T., 2003. Relationship between Indosinian–Yanshanian tectonic framework and large–superlarge mineral deposits in Qinling-Qilian Orogenic belt. Mineral Deposits, 22(01): 65–71 (in Chinese with English abstract).

Feng, C.Y., Feng, Y.D., Xu, J.X., Zeng, Z.L., She, H.Q., Zhang, D.Q., Qu, W.J., and Du, A.D., 2007a. Isotope chronological evidence for Upper Jurassic petrogenesis and mineralization of altered granite-type tungsten deposits in the Zhangtiantang area, southern Jiangxi. Geology in China, 34(04): 642–650 (in Chinese with English abstract).

Feng, C.Y., Li, D.S., Qu, W.J., Du, A.D., Wang, S., Su, S.S., and Jiang, J.H., 2009. Re-Os isotopic dating of molybdenite from the Suolajier skarn-type copper-molybdenum deposit of Qimantage mountain in Qinghai province and its geological significance. Rock and Mineral Analysis, 28(03): 223–227 (in Chinese with English abstract).

Feng, C.Y., Xu, J.X., Zeng, Z.L., Zhang, D.Q., Qu, W.J., She, H.Q., Li, J.W., Li, D.X., Du, A.D., and Dong, Y.J., 2007b. Zircon SHRIMP U-Pb and molybdenite Re-Os dating in Tianmenshan—Hongtaoling tungsten-tin Orefield, Southern Jiangxi province, China, and its geological implication. Acta Geologica Sinica, 81(07): 952–963 (in Chinese with English abstract).

Feng, C.Y., Zeng, Z.L., Qu, W.J., Zhang, D.Q., and Wang, S., 2010. Discussion on metallochronology and time difference of diagenesis and mineralization of tungsten deposit in southern Jiangxi province. Mineral Deposits, 29(S1): 431–432 (in Chinese).

Gong, H.J., Zhu, L.M., Sun, B.Y., Li, B., Guo, B., and Wang, J.Q., 2009a. Zircon U-Pb age and Hf isotopic composition of the Dongjiangkou granitic pluton and its mafic enclaves in the South Qinling terrain. Acta Petrologica Sinica, 25(11): 3029–3042 (in Chinese with English abstract).

Gong, H.J., Zhu, L.M., Sun, B.Y., Li, B., and Guo, B., 2009b. Zircon U-Pb age and Hf isotopic characteristics and their geological significance of the Shahewan, Caoping and Zhashui granitic pluton in the South Qinling orogen. Acta Petrologica Sinica, 25(02): 248–264 (in Chinese with English abstract).

Hou, Z.Q., Qu, X.M., Wang, S.X., Gao, Y.F., Du, A.D., and Huang, W., 2003. Re-Os age of molybdenite in the Gangdese porphyry copper deposit, Tibet Plateau: Application of mineralization time and dynamic background. Science in China (Series D), 33(07): 609–618 (in Chinese).

Hu, J.M., Cui, J.T., Meng, Q.R., and Zhao, C.Y., 2004. The U-Pb age of zircons separated from the Zhashui granite in Qinling orogen and its significance. Geological Review, 50(03): 323–329 (in Chinese with English abstract).

Huang, D.H., Wu, C.Y., Du, A.D., and He, H.L., 1994. Re-Os isotopic age of molybdenum deposits in east Qinling and their significance. Mineral Deposits, 13(03): 221–230 (in Chinese with English abstract).

Huang, D.H., Du, A.D., Wu, C.Y., Liu, L.S., Sun, Y.L., and Zou, X.Q., 1996. Metallochronology of molybdenum (-copper) deposits in the north China platform: Re-Os age of molybdenite and its geological significance. Mineral Deposits, 15(04): 365–373 (in Chinese with English abstract).

Huang, X.E., 2009. New discoveries and revelations of prospecting tungsten deposits in China. China Tungsten Industry, 24(05): 33–37 (in Chinese with English abstract).

Jiang, Y.H., Jin, G.D., Liao, S.Y., Zhou, Q., and Zhao, P., 2010. Geochemical and Sr-Nd-Hf isotopic constraints on the origin of late Triassic granitoids from the Qinling orogen, central China: Implications for a continental arc to continent-continent collision. Lithos, 117(1–4): 183–197.

Kang, Y.F., 1959. Achievements and experience in tungsten geological exploration in central and southern China in the past decade. Geology and Exploration, (19): 3–7 (in Chinese).

Li, C., Qu, W.J., and Du, A.D., 2009b. Comprehensive study on extraction of Rhenium with acetone in Re-Os isotopic dating. Rock and Mineral Analysis, 28(3): 233–238.

Li, C., Qu, W.J., Zhou, L.M., and Du, A.D., 2010b. Rapid separation of osmium by direct distillation with carius tube. Rock and Mineral Analysis, 29(1): 14–16.

Li, C., Yang, X., Zhao, H., Zhou, L.M., Du, A.D., Li, X.W., and Qu, W.J., 2015b. High precise isotopic measurements of pg-ng Os by negative ion thermal ionization mass spectrometry. Rock and Mineral Analysis, 34(4): 392–398.

Li, C.Y., Wang, F.Y., Hao, X.L., Ding, X., Zhang, H., Ling, M.X., Zhou, J.B., Li, Y.L., Fan, W.M., and Sun W.D., 2012. Formation of the world's largest molybdenum metallogenic belt: A plate-tectonic perspective on the Qinling molybdenum deposits. International Geology Review, 54(9): 1093–1112.

Li, H.M., Ye, H.S., Mao, J.W., Wang, D.H., Chen, Y.C., Qu, W.J., and Du, A.D., 2007. Re-Os dating of molybdenites from Au (-Mo) deposits in Xiaoqinling gold ore district and its geological significance. Mineral Deposits, 26(04): 417–424 (in Chinese with English abstract).

Li, H.Y., Mao, J.W., Sun, Y.L., Zou, X.Q., He, H.L., and Du, A.D., 1996. Re-Os isotopic chronology of molybdenites in the Shizhuyuan polymetallic tungsten deposit, southern Hunan. Geological Review, 42(03): 261–267 (in Chinese with English abstract).

Li, J.M., 2009. On the characteristics and utilization of China's Tungsten Resources. China Tungsten Industry, 24(06): 9–13 (in Chinese with English abstract).

Li, N., Chen, Y.J., Santosh M., and Franco P., 2015a. Compositional polarity of Triassic granitoids in the Qinling orogen, China: Implication for termination of the northernmost paleo-Tethys. Gondwana Research, 27(1): 244–257.

Li, S.Q., Yang, X.Y., Qu, W.J., Chen, F.K., and Sun, W.D., 2010a. Molybdenite Re-Os age and metallogeny of the Yueheping skarn molybdenum deposit in Ningshan, southern Qinling. Acta Petrologica Sinica, 26(05): 1479–1486 (in Chinese with English abstract).

Li, Y.F., Mao, J.W., Bai, F.J., Li, J.P., and He, Z.J., 2003. Re-Os isotopic dating of molybdenites in the Nannihu molybdenum (tungsten) orefield in the eastern Qinling and its gological significane. Geological Review, 49(06): 652–659 (in Chinese with English abstract).

Li, Y.F., Mao, J.W., Liu, D.Y., Wang, Y.B., Wang, Z.L., Wang, Y.T., Li, X.F., Zhang, Z.H., and Guo, B.J., 2006. SHRIMP zircon U-Pb and molybdenite Re-Os dating for the Leimengou porphyry molybdenum deposit, western Henan and its geological implication. Geological Review, 52(01): 122–131 (in Chinese with English abstract).

Liu, Q., 2013. The characteristics and genesis of the Zhen'an W deposits, Shaanxi Province, China. China University of Geosciences (Beijing) (Master thesis): 1–75 (in Chinese with English abstract).

Liu, S.W., Yang, P.T., Li, Q.G., Wang, Z.Q., Zhang, W.Y., and Wang, W., 2011. Indosinian granitoids and orogenic processes in the middle segment of the Qinling orogen, China. Journal of Jilin University (Earth Science Edition), 41(06): 1928–1943 (in Chinese with English abstract).

Luo, J.C., Lai, S.C., Qin, J.F., Li, H.B., Li, X.J., and Zang, W.J., 2010. Geochemistry and geological significance of Late Triassic Yanzhiba pluton from the Southern Qinling orogenic belt. Geological Review, 56(06): 792–800 (in Chinese with English abstract).

Luo, Q.Z., Dai, X.Y., Li, X.L., Zhou, X.K., Du, S.X., Chen, G.C., and Zhang, J.L., 2007. Relationship between the Middle Cenozoic interacontinental orogenesis and mineralization in the Qinling orogenic belt (Shaanxi part). Geology of Shaanxi, 25(02): 25–30 (in Chinese with English abstract).

Mao, J.W., Chen, M.H., Yuan, S.D., and Guo, C.L., 2011a. Geological characteristics of the Qinhang metallogenic belt in South China and spatial-temporal distribution regularity of mineral deposits. Acta Geologica Sinica, 85(05): 636–658 (in Chinese with English abstract).

Mao, J.W., Franco, P., and Nigel, C., 2011b. Mesozoic metallogeny in East China and corresponding geodynamic settings—An introduction to the special issue. Ore Geology Reviews, 43(1): 1–7.

Mao, J.W., Xie, G.Q., Zhang, Z.H., Li, X.F., Wang, Y.T., Zhang, C.Q., and Li, Y.F., 2005. Mesozoic large-scale metallogenic pulses in North China and corresponding geodynamic settings. Acta Petrologica Sinica, 21(01): 169–188 (in Chinese with English abstract).

Mao, J.W., Xie, G.Q., Guo, C.L., and Chen, Y.C., 2007. Large-scale tungsten-tin mineralization in the Nanling region, South China: Metallogenic ages and corresponding geodynamic processes. Acta Petrologica Sinica, 23(10): 2329–2338 (in Chinese with English abstract).

Mao, J.W., Xie, G.Q., Cheng, Y.B., and Chen, Y.C., 2009a. Mineral deposit models of Mesozoic ore deposits in South China. Geological Review, 55(03): 347–354 (in Chinese with English abstract).

Mao, J.W., Yang, J.M., Zhang, Z.H., Zhang, Z.C., Wang, Z.L., and Tian, F., 2000. The study on petrology, mineralogy and geochemistry of tungsten-bearing granitic rocks in the Yeniutan, Subei county, Gansu province. Acta Geologica Sinica, 74(02): 142–155 (in Chinese with English abstract).

Mao, J.W., Ye, H.S., Wang, R.T., Dai, J.Z., Jian, W., Xiang, J.F., Zhou, K., and Meng, F., 2009b. Mineral deposit model of Mesozoic porphyry Mo and vein-type Pb-Zn-Ag ore deposits in the eastern Qinling, central China and its implication for prospecting. Geological Bulletin of China, 28(01): 72–79 (in Chinese with English abstract).

Mao, J.W., Zhang, Z.C., Zhang, Z.H., and Du, A.D., 1999a. Re-Os isotopic dating of molybdenites in the Xiaoliugou W (Mo) deposit in the northern Qilian Mountains and its geological significance. Geochimica et Cosmochimica Acta, 63(11–12): 1815–1818.

Mao, J.W., Zhang, Z.H., Zhang, Z.C., Yang, J.M., Wang, Z.L., and Du, A.D., 1999b. Re-Os age dating of molybdenites in the Xiaoliugou tungsten deposit in the northern Qilian Mountains and its significance. Geological Review, 45(4): 412–417 (in Chinese with English abstract).

Mc Candless, T.E., Ruiz, J.R., and Campbell, A.R., 1993. Rhenium behavior in molybdenite in hypogene and near-surface environments: Implications for Re-Os geochronometry. Geochimica et Cosmochimica Acta, 57(04): 889–905.

Meng, X.J., Hou, Z.Q., Gao, Y.F., Huang, W., Qu, X.M., and Qu, W.J., 2003. Re-Os dating for molybdenite from Qulong porphyry copper deposit in Gangdese metallogenic belt, Xizang and its metallogenic significance. Geological Review, 49(06): 660–666 (in Chinese with English abstract).

Nie, F.J., Jiang, S.H., Hu, P., and Zhang, Y., 2004. Geological features and ore-forming material sources of Hongjianbingshan tungsten deposit in Beishan mountain, Gansu province. Mineral Deposits, 23(01): 11–19 (in Chinese with English abstract).

Nier, A.O., 1937. The isotopic constitution of Osmium. Applied Physics Reviews, 52(8): 885–885.

Ping, X.Q., Zheng, J.P., Zhao, J.H., Tang, H.Y., and Griffin, W.L., 2013. Heterogeneous sources of the Triassic granitoid plutons in the southern Qinling orogen: An E–W tectonic division in Central China. Tectonics, 32(3): 396–416.

Qin, J.F., 2010. Petrogenesis and geodynamic implications of the Late-Triassic granitoids from the Qinling orogenic belt. Northwest University (Ph.D thesis): 1–183 (in Chinese with English abstract).

Rollinson, H.R., 1993. Using geochemical data: Evaluation, presentation, interpretation. London: Longman, UK: 1–315.

Ruan, S.Q., Yang, X.K., Zhu, W., Gao, Y.F., and Han, K., 2019. Study on characteristics of ore-forming fluids in Qipangou tungsten mining area, western of Zhen'an, Shaanxi. Gold Science and Technology, 27(02): 153–162 (in Chinese with English abstract).

Sheng, J.F., Chen, Z.H., Liu, L.J., Ying, L.J., Huang, F., Wang, D.H., Wang, J.H., and Zeng, L., 2015. Outline of metallogeny of tungesten deposits in China. Acta Geologica Sinica, 89(06): 1038–1050 (in Chinese with English abstract).

Stein, H.J., Markey, R.J., Morgan, J.W., Hannah, J.L., and Schersten, A., 2001. The remarkable Re-Os chronometer in molybdenite: How and why it works. Terra Nova, 13(06): 479–486.

Sun, W.D., Li, S.G., Chen, Y.D., and Li, Y.J., 2000. Zircon U-Pb dating of granitoids from South Qinling, central China and their geological significance. Geochimica, 29(03): 209–216 (in Chinese with English abstract).

Sun, W.L., Niu, Y.L., Ma, Y.X., Liu, Y., Zhang, G.R., Hu, Z.X., Zhang, Z.W., Chen, S., Li, J.Y., Wang, X.L., and Gong, H.M., 2015. Petrogenesis of the Chagangnuoer deposit, NW China: A general model for submarine volcanic-hosted skarn iron deposits. Science Bulletin, 60(3): 363–379.

Wang, J.H., Zhang, F.X., Yu, Z.P., and Yu, L., 2002. Minerogenetic series of metallic ore deposits in the Qinling Mountains and tectonodynamic background of the continental orogenic belts. Geology in China, 29(02): 192–196 (in Chinese with English abstract).

Wang, J.M., Cao, H.Y., Dong, S.Q., Zhu, M., Shi, L.Y., Dang, C., and You, J., 2017. Genetic discussion and geological and characteristics of geochemical of Jinpen tungsten deposit in Zhen'an, Shaanxi Province. Science Technology and Engineering, 17(30): 1–8 (in Chinese with English abstract).

Wang, P.A., and Chen, Y.C., 1997. Tectono-minerogenic cycles and minerogenetic evolution through geological history in the Qinling orogenic belt. Journal of Geomechanics, 3(01): 10–20 (in Chinese with English abstract).

Wang, X.X., Wang, T., Qi, Q.J., and Li, S., 2011. Temporal-spatial variations, origin and their tectonic significance of the Late Mesozoic granites in the Qinling, Central China. Acta Petrologica Sinica, 27(06): 1573–1593 (in Chinese with English abstract).

Wei, L.M., Yang, Y.Z., Zhang, H., He, J.F., and Chen, F.K., 2016. Petrogenesis of Yanzhiba granite in South Qinling: Constraints from zircon U-Pb ages, geochemistry and Sr-Nd-Pb isotope. Journal of Earth Sciences and Environment, 38 (04): 527–546 (in Chinese with English abstract).

Xiao, X., Zhou, T.F., Yuan, F., Fan, Y., Zhang, D.Y., Liu, D.Z., Huang, W.P., and Chen, X.F., 2017. The geochronology of the Qingyang Gaojiabang tungsten-molybdenum deposit and its geological significance, Anhui Province, East China. Acta Petrologica Sinica, 33(03): 859–872 (in Chinese with English abstract).

Xu, J.X., Zeng, Z.L., Wang, D.H., Chen, Z.H., Liu, S.B., Wang, C.H., and Ying, L.J., 2008. A new type of tungsten deposit in

southern Jiangxi and the new model of "Five Floors +Basement" for prospecting. Acta Geologica Sinica, 82(07): 880–887 (in Chinese with English abstract).
Xu, K.Q., and Cheng, H., 1987. Tectonic environment for the formation of tungsten deposits in China. Contributions to Geology and Mineral Resources Research, 2(03): 1–7 (in Chinese with English abstract).
Yan, Z., Wang, Z.Q., Chen, L., Liu, S.W., Ren, T., Xu, X.Y., and Wang, R.T., 2014. Tectono-magmatism and metallogeneses of Shanyang-Zhashui ore concentration area in Qinling Orogen. Acta Petrologica Sinica, 30(2): 401–414 (in Chinese with English abstract).
Yang, K., Liu, S.W., Li, Q.G., Wang, Z.Q., Han, Y.G., Wu, F.H., and Zhang, F., 2009. LA-ICP-MS zircon U-Pb geochronology and geological significance of Zhashui granitoids and Dongjiangkou granitoids from Qinling, central China. Acta Scientiarum Naturalium Universitatis Pekinensis, 45(05): 841–847 (in Chinese with English abstract).
Yang, P.T., Liu, S.W., Li, Q.G., Zhang, F., Wang, Z.Q., Wang, D.S., Wang, R.T., Yan, Q.R., and Yan, Z., 2011. Ages of the Laocheng granitoids and crustal growth in the South Qinling tectonic domain, Central China: Zircon U-Pb and Lu-Hf isotopic constraints. Acta Geologica Sinica (English Edition), 85(4): 854–869.
Yao, S.Z., Ding, Z.J., Zhou, Z.G., and Chen, S.Y., 2002. Metallogenic system of Qinling orogen. Earth Science-Journal of China University of Geosciences, 27(05): 599–604 (in Chinese with English abstract).
Ye, H.S., Mao, J.W., Li, Y.F., Guo, B.J., Zhang, C.Q., Liu, J., Yan, Q.R., and Liu, G.Y., 2006. SHRIMP zircon U-Pb and molybdenite Re-Os dating for the superlarge Donggou porphyry Mo deposit in east Qinling, China, and its geological implication. Acta Geologica Sinica, 80(07): 1078–1088 (in Chinese with English abstract).
Zhang, B.L., Jia, W.C., Shen, X.L., Guo, Z.H., Huang, X.F., and Xu, Y.S., 2010. The northern orogenic belt tungsten distribution, type, age and tectonic setting. Mineral Deposits, 29(S1): 327–328 (in Chinese).
Zhang, C.L., Wang, T., and Wang, X.X., 2008. Origin and tectonic setting of the early Mesozoic granitoids in Qinling orogenic belt. Geological Journal of China Universities, 14 (03): 304–316 (in Chinese with English abstract).
Zhang, D.Y., Zhou, T.F., Yuan, F., Fan, Y., Liu, S., and Qu, W.J., 2009. A genetic analysis of Baishan molybdenum deposit in East Tianshan area, Xinjiang. Mineral Deposits, 28 (05): 663–672 (in Chinese with English abstract).
Zhang, G.W., Cheng, S.Y., Guo, A.L., Dong, Y.P., Lai, S.C., and Yao, A.P., 2004. Mianlue paleo-suture on the southern margin of the central orogenic system in Qinling-Dabie with a discussion of the assembly of the main part of the continent of China. Geological Bulletin of China, 23(9–10): 846–853 (in Chinese with English abstract).
Zhang, G.W., Dong, Y.P., and Yao, A.P., 2001. Review on the development of studies on the tectonic and orogen process of orogenic belt, and discussing on some new key problems. Northwestern Geology, 34(01): 1–9 (in Chinese with English abstract).
Zhang, G.W., Meng, Q.R., and Lai, S.C., 1995. Tectonics and structure of Qinling orogenic belt. Science in China (Series B), 25(09): 994–1003 (in Chinese).
Zhang, H., Chen, D.L., Zhai, M.G., Zhang, F.X., Gong, X.K., and Sun, W.D., 2015. Molybdenite Re-Os dating and its tectonic significance of the Guilingou porphyry molybdenum deposit, southern Qinling. Acta Petrologica Sinica, 31(07): 2023–2037 (in Chinese with English abstract).
Zhang, Z.Q., Zhang, G.W., Liu, D.Y., Wang, Z.Q., Tang, S.H., and Wang, J.H., 2006. Isotopic geochronology and geochemistry of ophiolites, granites and clastic sedimentary rocks in the Qinling Orogenic Belt. Beijing: Geological Publishing House: 1–348 (in Chinese).
Zhou, X.K., Wang, G.Q., Liu, X.W., Du, S.X., Guo, P.Y., Guo, Q.M., and Li, Z.N., 2016. Contrast between the petrochemical characteristics of Wangjiaping concealed ore body and the typical tungsten mineralization of granite in south China. Geology of Shaanxi, 34(02): 41–46 (in Chinese with English abstract).
Zhu, L.M., Zhang, G.W., Li, B., and Guo, B., 2008. Main geological events, genetic types of metallic deposits and their geodynamical setting in the Qinling orogenic belt. Bulletin of Mineralogy, Petrology and Geochemistry, 27(04): 384–390 (in Chinese with English abstract).
Zhu, L.M., Zhang, G.W., Guo, B., Ben L., Gong, H.J., and Wang, F., 2010. Geochemistry of the Jinduicheng Mo-bearing porphyry and deposit, and its implications for the geodynamic setting in East Qinling, P.R. China. Chemie der Erde, 70(02): 159–174.
Zhu, L.M., Zhang, G.W., Li, B., Guo, B., Yao, A.P., and Gong, H.J., 2009. Some key metallogenic events of Qinling orogenic belt and their deposit examples. Journal of Northwest University (Natural Science Edition), 39(03): 381–391 (in Chinese with English abstract).

About the first author

HAN Ke, male, born in 1990 in Shaanxi Province, is currently a doctoral candidate at the School of Earth Science and Resources, Chang'an University. His research interests focus on metallic ore deposit and orefield structure using orefield structure-alteration facies mapping and geochronology for mineral prospecting and mineralization mechanism. E-mail: 877415765@qq.com.

About the corresponding author

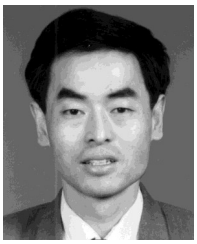

YANG Xingke, male, born in 1961 in Shaanxi Province, professor at the School of Earth Science and Resources, Chang'an University. His academic interests focus on tectonic geology, orefield structure and metallogenic prediction. E-mail: xky61@163.com.